Bioorg. Med. Chem. 44 (2021) 116283

Contents lists available at ScienceDirect

Bioorganic & Medicinal Chemistry

journal homepage: www.elsevier.com/locate/bmc

Fragment-based lead discovery to identify novel inhibitors that target the ATP binding site of pyruvate dehydrogenase kinases

Tatsuo Akaki [a,*], Yuki Bessho [a], Takashi Ito [a], Shingo Fujioka [a], Minoru Ubukata [a], Genki Mori [a], Kenji Yamanaka [b], Takuya Orita [a], Satoki Doi [a], Tomoko Iwanaga [a], Kazutaka Ikegashira [a], Yoshiji Hantani [b], Isao Nakanishi [c], Tsuyoshi Adachi [a]

[a] Chemical Research Laboratories, Central Pharmaceutical Research Institute, Japan Tobacco Inc, 1-1, Murasaki-cho, Takatsuki, Osaka 569-1125, Japan
[b] Biological/Pharmacological Research Laboratories, Central Pharmaceutical Research Institute, Japan Tobacco Inc, 1-1, Murasaki-cho, Takatsuki, Osaka 569-1125, Japan
[c] Computational Drug Design and Discovery, Department of Pharmaceutical Sciences, Kindai University, 3-4-1, Higashi-osaka, Osaka 577-8502, Japan

ARTICLE INFO

Keywords:
Fragment-based drug discovery (FBDD)
X-ray fragment hit
Pyruvate Dehydrogenase Kinases (PDHKs)
ATP binding site

ABSTRACT

A fragment-based lead discovery approach was applied to Pyruvate Dehydrogenase Kinases (PDHKs) to discover inhibitors against the ATP binding site with novel chemotypes. X-ray fragment screening toward PDHK4 provided a fragment hit **1** with a characteristic interaction in a deep pocket of the ATP binding site. While known inhibitors utilize several water molecules in a deep pocket to form water-mediated hydrogen bond interactions, the fragment hit binds deeper in the pocket with a hydrophobic group. Displacement of a remaining water molecule in the pocket led to the identification of lead compound **7** with a notable improvement in inhibition potency. This lead compound possessed high ligand efficiency (LE) and showed decent selectivity profile. Two additional lead compounds **10** and **13** with new scaffolds with tricyclic and bicyclic cores were generated by merging structural information of another fragment hit **2**. The characteristic interaction of these novel inhibitors in a deep pocket provides new structural insights about PDHKs ATP binding site and opens a novel direction for the development of PDHKs inhibitors.

1. Introduction

The human pyruvate dehydrogenase complex (PDC) catalyzes the oxidative decarboxylation of pyruvate with formation of acetyl-CoA. PDC activity is regulated by pyruvate dehydrogenase kinase (PDHK), which phosphorylates and inactivates PDC. The reduction of PDC activity, which is caused by the induction and activation of PDHK, have been observed in various diseases such as type 2 diabetes, ischemic heart disease, peripheral artery disease, pulmonary hypertension, and cancers.[1–6] There are four isozymes of PDHK (PDHK1, 2, 3, and 4),[7] and it has been reported that the glucose levels of PDHK2/4 double knockout mice are lower than single knockout mice bearing only PDHK2 or PDHK4.[8] It is also known that the expression levels of PDHKs are higher in patients with the diseases mentioned above.

To suppress four isozymes of PDHK, we have started our research program targeting the isoform conserved ATP binding site. Fig. 1 shows some examples of known PDHK inhibitors against the ATP binding site, and these known ATP-binders inhibit all PDHK isozymes. [9–12]

Fig. 2 shows the AMP-PNP bound X-ray structure of PDHK4.[13] The ATP binding site is located in the *N*-terminal domain of PDHKs. PDHK is a member of the GHKL ATPase kinase superfamily, and like other GHKL family proteins, the adenine binding site includes four conserved water molecules. WAT1, which bridges Asp293 and the adenine ring, is a structural water as it forms four hydrogen bonds. Three other conserved water molecules are involved in a hydrogen bond network in a deeply buried pocket, mediating interactions with the nearby Leu255, Asn258, Ile291, and Asp293 residues. Known inhibitors which bind at the adenine binding site utilize several water molecules to form a water-mediated interaction in the deep pocket. The resorcinol core, which is frequently used as a GHKL ATPase inhibitor as in the case of PDHK, replaces one water molecule (WAT4) with one phenolic hydroxyl group that is involved in a hydrogen bond network. The loop consisting of residues 317–330, known as the 'ATP lid' trapping the ATP phosphate, is partially visible in the electron density of the X-ray structure.

* Corresponding author.
E-mail address: tatsuo.akaki@jt.com (T. Akaki).

https://doi.org/10.1016/j.bmc.2021.116283
Received 13 April 2021; Received in revised form 13 June 2021; Accepted 17 June 2021
Available online 8 July 2021

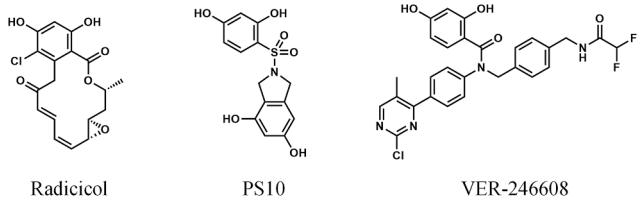

Fig. 1. PDHK inhibitors actting at ATP site.

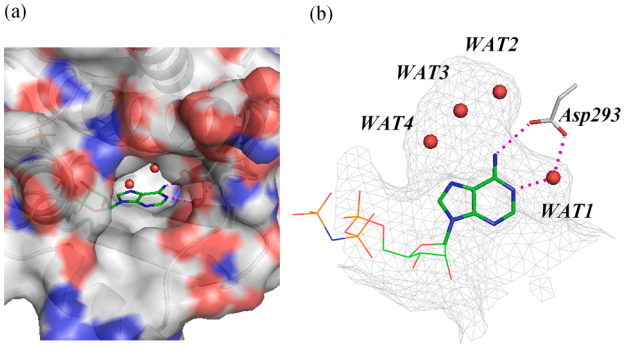

Fig. 2. X-ray Structure of AMP-PNP bound on PDHK4. (PDB ID: 2E0A). (a) Protein surface is coloured with red oxygen, blue nitrogen, yellow sulfur and gray carbon atoms. AMP-PNP is shown in sticks with light green carbons. Water molecules are represented as red spheres, and dashed lines indicate hydrogen bonds. (b) Detailed view around adenine binding site. Protein interiors are shown in gray mesh. Four water molecules (red spheres) are coordinated in the binding pocket.

To find novel chemotypes of inhibitors that target the ATP binding site of PDHKs, we applied a fragment-based drug discovery (FBDD) strategy. FBDD has emerged as an effective methodology to identify new chemotypes utilizing low-molecular-weight fragments.[14] As the probability of fitting into the binding pocket falls dramatically for a bigger sized compound, FBDD generally gives a higher hit rate compared to traditional high-throughput screening. As the affinities of the fragment hits are weak, optimization is generally carried out utilizing X-ray structural information so that the affinity is increased effectively. Higher hit rates followed by the rapid affinity increase with structural information makes the fragment-based lead discovery approach a potential strategy to gain novel chemotypes.

In this report, we describe our FBDD process leading to the generation of lead compounds with novel chemotypes at the PDHK ATP binding site.

2. Results and discussion

2.1. Identification of fragment hits with novel chemotypes from X-ray fragment screening

X-ray fragment screening was applied to discover novel chemotypes of binders against the ATP binding site of PDHKs. X-ray fragment screening toward PDHK4 using our in-house fragment library of 638 fragments led to the identification of 17 fragment hits, corresponding to a hit rate of 2.66%. All these fragments were found to bind on the ATP site. Among the gained fragment hits, compounds **1** and **2** were selected for further structure-guided medicinal chemistry (Fig. 3). These compounds showed a clear binding pose at the ATP binding site in the X-ray structure. Fragment **1** participated in a hydrogen-bonding network with Asp293 and the structural water molecule (WAT1) through an amide of the lactam core, and showed characteristic interaction in a deep pocket. While known inhibitors like VER-246608 keep at least WAT2 and WAT3

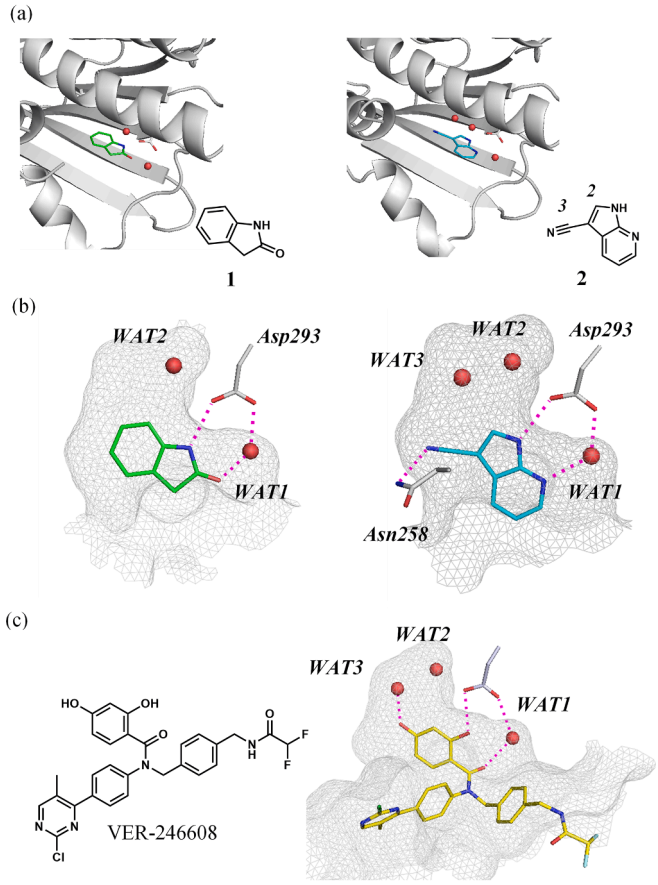

Fig. 3. Selected fragment hits from X-ray screening toward PDHK4. (a) PDHK4 is shown in gray cartoons. The fragment hits are shown in sticks with light green carbons for **1** and cyan carbons for **2**. Location number is indicated in italic on compound **2**. (b) Detailed view around fragment binding site. Protein interiors are shown in gray mesh. Water molecules are represented as red spheres, and dashed lines indicate hydrogen bonds. (c) X-ray structure of a resorcinol ligand bound on PDHK2 (PDB ID: 4V25). VER-246608 is shown in sticks with yellow carbons.

conserved water molecules in the deep pocket to form water-mediated hydrogen bond interactions with surrounding residues, fragment **1** binds deeper by displacing the WAT3 and WAT4 conserved waters. The phenyl ring of fragment **1** displaced these waters without forming hydrogen-bond interaction with surrounding residues. Fragment **2** also participated in a hydrogen-bonding network with Asp293 and WAT1, The cyano group displaces one conserved water molecule (WAT4) to form a hydrogen-bond interaction with Asn258. The hydrogen at the 2-position of fragment **2** is in close contact with WAT3 to form a CH-O interaction, and the 3-position cyano group is considered to strengthen this interaction through an inductive effect. Inhibition activity of these fragment hits was measured by a RapidFire mass assay which detected the PDH reaction product acetyl-coenzyme A, and these hits did not show measurable inhibition activity at levels up to 1000 μM on PDHK4. X-ray structures of PDHK2 with these fragment hits were also obtained, and similar binding poses were observed for each fragment (PDB codes: see the later "Accession codes" section).

2.2. SBDD optimization of fragment hit 1 into a lead compound

Firstly, a structure-based design approach was applied to fragment hit **1** to improve PDHKs inhibition activity. Analysis of the X-ray structure of **1** with PDHK4 revealed that there is a hydrophobic space around Ile303 (Fig. 4). Compound **3** was purchased to fulfill the space with a Me

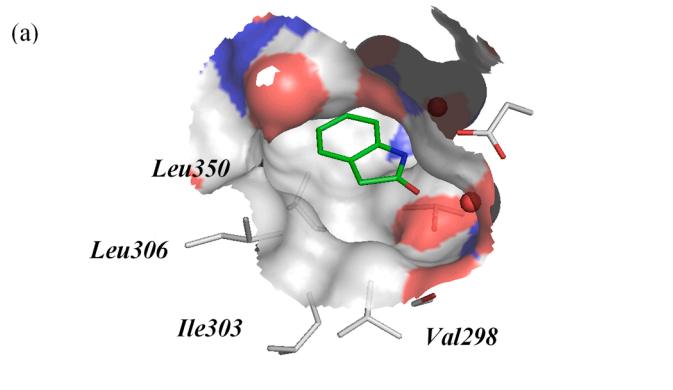

Fig. 4. (a) Detailed View around Ile303 of X-ray structure of **1** with PDHK4. Protein surface is coloured with red oxygen, blue nitrogen, yellow sulfur and gray carbon atoms. Compound **1** is shown in sticks with light green carbons. (b) PDHK2 and PDHK4 IC_{50} were determined by RapidFireMass Spectroscopy. Location number is indicated in italic on compound **1**. (c) Values in parthness were percent inhibition at the indicated concentration.

substituent from the 3-position of the lactam core, and exhibited an increased activity in the RapidFire mass assay (PDHK2 IC_{50} = 50.2 μM, PDHK4 IC_{50} = 890 μM).

To further improve the inhibition activity, hydration site analysis using the WaterMap[15] calculation was carried out on the compound **1** X-ray structure (Fig. 5). WaterMap is a molecular dynamics (MD)-based computational method to detect hydration sites from resultant MD trajectories, and also to calculate the thermodynamic properties (free energy (ΔG), enthalpy (ΔH) and entropy (-TΔS)) relative to bulk water. The WaterMap calculation on the compound **1** X-ray structure reproduced the hydration sites at two conserved water positions (WAT1 and WAT2). The detected hydration site at the WAT1 position gave a stable free energy value (−0.37 kcal/mol) relative to the bulk water, and the hydration site at WAT2 position gave unstable free energy (+7.11 kcal/mol). The thermodynamic profile at the WAT2 position was calculated as both enthalpy and entropy values that were unstable relative to the bulk water (enthalpy =+3.99 kcal/mol, entropy = +3.12 kcal/mol). Water molecules at the WAT2 position in MD trajectories are within hydrogen bonding distance with the Asp293 sidechain, The358 backbone, and Ile291 backbone, and as Thr358 and Ile291 are in the β-sheet, hydrogen bond geometries with these residues are far from ideal. The unstable enthalpic energy profile on the WAT2 position suggested that the polar interaction on this hydration site was not enough to overcome the desolvation penalty of the bound ligand. The thermodynamic profile of the WaterMap calculation result led to the strategy to hold stable the conserved water molecule (WAT1), and to displace another unstable water molecule (WAT2) with a hydrophobic group.

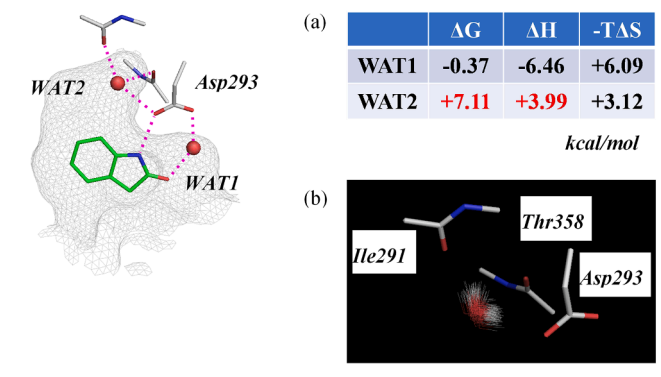

	ΔG	ΔH	-TΔS
WAT1	-0.37	-6.46	+6.09
WAT2	+7.11	+3.99	+3.12

kcal/mol

Fig. 5. WaterMap calculation of comp **1** X-ray structure on PDHK4. (a) Thermodynamic profile of WaterMap detected two hydration sites. Free energy (ΔG), enthalpy (ΔH) and entropy (-TΔS) relative to a bulk water were calculated through MD calculation. (b) MD trajectories of the water molecule at WAT2 hydration site.

The crystal structure of compound **1** indicated that the 7-position of the lactam core was the ideal position for attaching substituents to displace the unstable WAT2 water. Table 1 shows the SAR result of installing several chemical groups at the R_1 position. Compound **4** and **5** were designed to displace the WAT2 water molecule with the alkyl groups. A methyl aniline compound **7** was designed to displace the WAT2 water with a methyl substituent, and to form an additional hydrogen bond interaction with Asp293. A primary aniline compound **6** was also synthesized to form a hydrogen bond interaction with Asp293. The inhibitory activities toward PDHK2 and PDHK4 were measured by spectrophotometric assay which detected the residual PDH activity by measuring the absorbance of NADH at 340 nm. Ethyl compound **4** improved the potency by 20-fold against PDHK2, and cyclopropyl compound **5** also showed moderate inhibitory activity. Methyl amine compound **7** further improved the potency which showed IC_{50} values 0.59 μM and 12.8 μM against PDHK2 and PDHK4, respectively. As the activity of the amine compound **6** was very weak (PDHK2 and PDHK4 IC_{50} > 300 μM), this demonstrates the importance of the methyl substituent of compound **7**.

Compound **7** was selected as a lead compound and several profiles were measured. PDHK1 and PDHK3 inhibition activities were measured for **7**, and ligand efficiency was derived for all PDHK isozymes (Table 2). Compound **7** inhibited all PDHK isozymes and possessed high ligand efficiency.

To evaluate the selectivity profile of lead compound **7**, inhibition assays toward other GHKL family proteins and a kinase panel assay were conducted (Table 3). BCKDK and HSP90 were selected from GHKL family proteins, because BCKDK has the highest sequence similarity to PDHKs, and some PDHKs inhibitors were reported to inhibit HSP90[10]. The fluorescence polarization assay using labeled geldanamycin was used for HSP90, the luminescent assay using ADP-Glo™ was used for BCKDK inhibition assay, and DiscoverX KINOME scan™ was used for the protein kinase panel assay. Compound **7** showed little inhibition on HSP90 and BCKDK, and in the DiscoveRx KINOME scan™ assay, showed more than 50% inhibition for just 2 kinases of MTOR and MAST1 among 59 kinases at 10 μM. These data demonstrate the decent selectivity profile of lead compound **7**.

The X-ray structure of **7** bound to PDHK4 was obtained and

Table 1
Influence of R_1 substituent on PDHK2 and PDHK4 activity.[a]

	compound	R_1	PDHK2 IC_{50} (μM)	PDHK4 IC_{50} (μM)
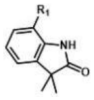	**3**	H	279	>300 (8.0%) [b]
	4		11.0	>300 (50%) [b]
	5		4.9	43.6
	6		>300 (47%) [b]	>300 (40%) [b]
	7		0.59	12.8

[a] PDHK2 and PDHK4 IC_{50} determined by absorption spectrophotometry method.
[b] Values in parentheses were percent inhibition at the indicated concentration.

Table 2
Inhibition activity and ligand efficiency of compound **7** toward all PDHK isozymes.

Target	IC_{50}	LE	Target	IC_{50}	LE
PDHK1	0.37 μM	0.63	PDHK3	8.4 μM	0.50
PDHK2	0.59 μM	0.61	PDHK4	12.8 μM	0.48

All PDHKs IC_{50} determined by absorption spectrophotometry method.

Table 3
Selectivity profile of compound **7.**; GHKL family assay and kinase panel assay result.

Family	Target	Inhibition percentage
GHKL	HSP90	3.2% at 30 μM [a]
	BCKDK	14% at 500 μM [b]
Protein Kinase [c]	44 kinases	<20% at 10 μM
	13 kinases	20–50% at 10 μM
	MTOR	58% at 10 μM
	MAST1	60% at 10 μM

[a] Fluorescence Polarization assay using labeled geldanamycin with BPS Bioscience assay kits.
[b] Luminescent kinase assay using ADP-Glo™.
[c] Kinase panel assay was conducted with DiscoverX KINOMEscan™ toward 59 kinases. For details, see the supporting information.

confirmed our design hypothesis (Fig. 6). The carbonyl oxygen keeps the WAT1-mediated hydrogen bond interaction with Asp293 of fragment hit **1**, and one methyl group at the alpha position of the carbonyl occupies the hydrophobic space around Ile303. The aniline NH of compound **7** formed a polar interaction with the Asp 293 sidechain. The methyl substituent on aniline, which boosted the activity of compound **7** from compound **6**, displaced the WAT2 water molecule in the buried pocket. For a primary aniline compound **6**, one hydrogen atom on the aniline substituent is considered to form a polar interaction with Asp 293 sidechain like **7**. The second aniline hydrogen is short in length to displace the WAT2 water molecule, and by superposing the WaterMap MD trajectories at WAT2 position, the geometry is far from ideal to form a hydrogen bond interaction with the remaining WAT2 molecule. Based on these results, large activity difference between compound **6** and **7** is considered to arise from the difference of WAT2 energy profile after the ligand binding.

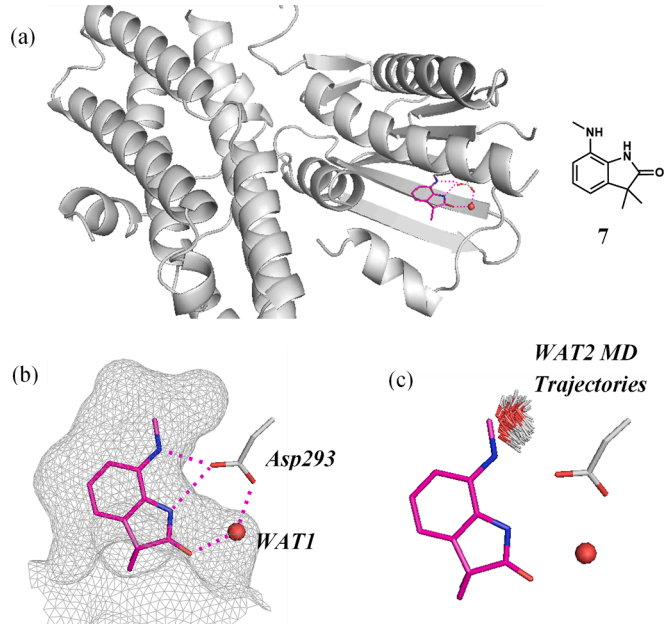

Fig. 6. X-ray Structure of compound **7** on PDHK4. (a) PDHK4 is shown in gray cartoons. The ligand is shown in sticks with pink carbons. Water molecules are represented as red spheres, and dashed lines indicate hydrogen bonds. (b) Detailed view around ligand binding site. Protein interiors are shown in gray mesh. (c) WaterMap MD trajectories of the water molecule at WAT2 hydration site on Fig. 5b are superimposed. The methyl substituent of compound **7** displaced the WAT2 position.

2.3. Generation of a new scaffold via merging lead compound 7 with fragment hit 2

The X-ray structure of fragment hit **2** was investigated to generate other lead compounds. The five-membered ring of compound **2** and lead compound **7** both interacts with Asp 293 of PDHK4, and by superimposing two X-ray structures of PDHK4, these rings overlay well (Fig. 7). From this overlay result, we undertook the design of a tri-cyclic core as a potential new scaffold.

The cyclopropyl substituent of compound **5** was used for a tricyclic core as a replacement for the methyl amine of compound **7** in view of the synthetic tractability, and compound **8** showed the same level of PDHK2 activity as the original compound **5** (Table 4). The weak PDHK4 activity of compound **8** could be attributed to a limited solubility in the assay buffer. Addition of a methyl substituent on the pyridine 2-position, which was designed to form CH-O interaction with Gly295 and Gly297 backbone carbonyl, led to improve activity of compound **9**. And by changing the core structure from pyridine to pyrimidine, pyrimidine **10** gave a low μM level IC_{50} inhibition activity for both PDHK2 and PDHK4. The selectivity toward BCKDK of the same GHKL family protein was evaluated for compound **10**, and this compound showed little inhibition.

To obtain further chemotypes of inhibitors, the structural and SAR information of the compound **7** and **10** were transferred into a bicyclic-core scaffold of fragment hit **2** (Fig. 8). The core structure of fragment hit **2** was changed from a pyridine to a 2-methyl pyrimidine, as the compound **10** improved activity from compound **8** by changing the core structure in this manner. In addition, to occupy the same space of terminal methyl of compound **7**, substituents with the chain length of three atoms were added at the R_1 position of the core structure.

Table 5 shows the SAR result of installing several chemical groups at the R_1, R_2, and R_3 positions on the bicyclic core. Addition of an *n*-Pr substituent on the R_1 position on compound **2** (compound **11**) led to a slight inhibition activity toward PDHK2. To fulfill the pocket interior with the hydrophobic group like compound **7** and **10**, the R_2 substituent was changed from cyano group to halogen and methyl, as in compounds **12**, **13**, and **14**. Compound **14** with a methyl substituent at R_2 position showed IC_{50} values of 14.7 μM for PDHK2, and compound **12** and **13** with halogen substituents further improved activity to a level of single micromolar IC_{50} for PDHK2. Attaching a chloride on the R_3 position slightly improved activity (from **14** to **15**). To further improve activity, we designed R_1 substituents to form an additional polar interaction with the aspartic acid moiety of PDHKs (Asp293 for PDHK4) as in the methyl amine of compound **7**. Methyl amide **16** and **17** were synthesized to form a hydrogen bond interaction with the aspartic acid moiety, but these compounds reduced the activity. Propenyl compound **18** was designed to form a CH-O interaction through alkene C—H, and this compound displayed sub 10μM IC_{50} values both for PDHK2 and PDHK4.

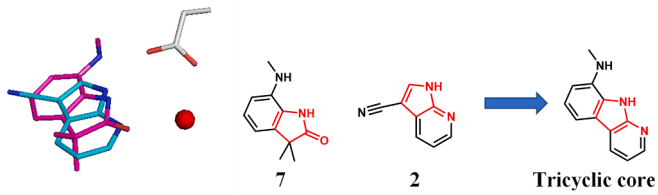

Fig. 7. Design strategy of the new tricyclic core scaffold. X-ray poses superimposition of a fragment hit **2** (cyan) and a lead compound **7** (purple).

Table 4

Inhibition activity of tricyclic cores on PDHK2 and PDHK4.[a]

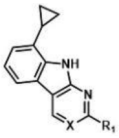

compound	X	R_1	PDHK2 IC_{50} (μM)	PDHK4 IC_{50} (μM)	BCKDK IC_{50} (μM) [b]
8	C	H	3.5	>300 (20%) [c]	
9	C	CH_3	2.0	12.0	
10	N	CH_3	0.71	5.9	>300 (3.0%) [c]

[a] PDHK2 and PDHK4 IC_{50} determined by absorption spectrophotometry method.
[b] Luminescent kinase assay using ADP-Glo™.
[c] Values in parentheses were percent inhibition at the indicated concentration.

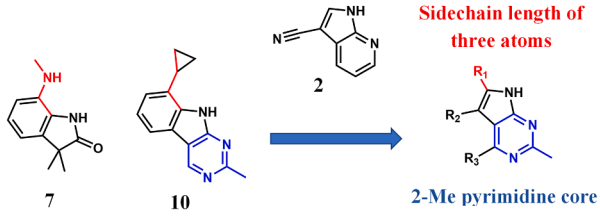

Fig. 8. Schematic representation of transferring compound **7** and **10** information on fragment hit **2**.

Table 5

Effect of R_1, R_2 and R_3 substituents on bicyclic pyrimidoindole core.

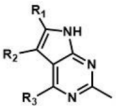

comp	R_1	R_2	R_3	PDHK2 IC_{50} (μM) [a]	PDHK4 IC_{50} (μM) [a]
11	*n*-Pr	CN	H	>30.0 (34%) [b]	>30.0 (8.5%) [b]
12	*n*-Pr	Cl	H	1.8	11.0
13	*n*-Pr	Br	H	2.2	12.4
14	*n*-Pr	CH_3	H	14.7	>30.0 (17%) [b]
15	*n*-Pr	CH_3	Cl	9.9	>30.0 (45%) [b]
16		CH_3	Cl	42.8	>100 (34%) [b]
17		Br	Cl	>30.0 (21%) [b]	>30.0 (3.1%) [b]
18		Cl	Cl	1.5	8.0

[a] PDHK2 and PDHK4 IC_{50} determined by absorption spectrophotometry method.
[b] Values in parentheses were percent inhibition at the indicated concentration.

Fig. 9 shows the X-ray co-crystal structure of compound **13** with PDHK2. The core keeps the hydrogen bond interaction with Asp290, which corresponds to Asp293 of PDHK4, and WAT1 of fragment hit **2**. The *n*-Pr and bromide substituents of **13** displaced all the three conserved interior water molecules.

2.4. Ligand efficiency of the obtained key compounds

Table 6 summarizes the inhibition activity and the ligand efficiency of the obtained key compounds. Inhibition activity of a commercially available resorcinol, methyl 2,4-dihydroxybenzoate, was also measured and displayed IC_{50} values of 192 μM for PDHK2 and 345 μM for PDHK4,

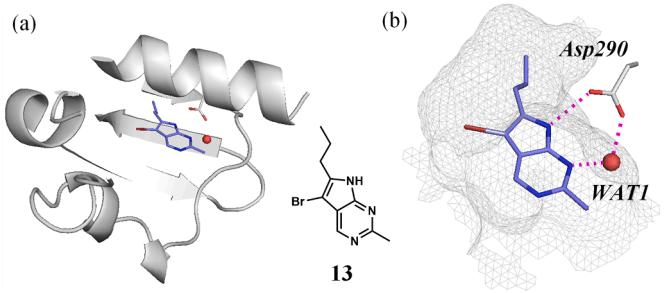

Fig. 9. X-ray Structure of compound **13** on PDHK2. (a) PDHK2 is shown in gray cartoons. The ligand is shown in sticks with purple carbons. (b) Detailed view around ligand binding site. Protein interiors are shown in gray mesh. Water molecules are represented as red spheres, and dashed lines indicate hydrogen bonds.

Table 6

Inhibition activity and ligand efficiency of key compounds.

compound	Number of Heavy Atoms	PDHK2 IC_{50} [a]and LE	PDHK4 IC_{50} [a] and LE
 methy 2,4-dihydroxybenzoate	12 Atoms	192 μM [b] (LE = 0.42)	345 μM [b] (LE = 0.39)
 **1**	10 Atoms	958 μM [b] (LE = 0.41)	>2000 μM [b]
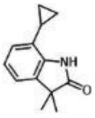 **5**	15 Atoms	4.9 μM (LE = 0.48)	43.6 μM (LE = 0.40)
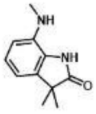 **7**	14 Atoms	0.59 μM (LE = 0.61)	12.8 μM (LE = 0.48)
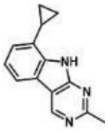 **10**	17 Atoms	0.71 μM (LE = 0.49)	5.9 μM (LE = 0.42)
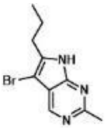 **13**	14 Atoms	2.2 μM (LE = 0.55)	12.4 μM (LE = 0.48)

[a] PDHK2 and PDHK4 IC_{50} determined by absorption spectrophotometry method.
[b] PDHK2 and PDHK4 IC_{50} determined by RapidFireMass Spectroscopy method.

corresponds to LE values of 0.42 and 0.39 respectively. A fragment hit **1** binds deeper from a resorcinol core in the pocket, and displayed a same level of LE value with the resorcinol toward PDHK2. LE values of compound **5** and **7** were improved from fragment hit **1** by displacing a conserved WAT2 water molecule interior. Compound **7** with a methyl amine substituent gave higher ligand efficiency compared to compound **5** with a cyclopropyl substituent, as the methyl amine forms an additional polar interaction with the aspartic acid moiety of PDHKs (Asp293 for PDHK4). Starting from X-ray fragment hit **1** with 10 heavy atoms, addition of 4 heavy atoms increased the PDHK2 activity more than 1000 times with **7**. For tricyclic series, weaker cyclopropyl substituent was used in view of the synthetic tractability, and compound **10** gave improved LE value from corresponding compound **5**. Compound **13** of bicyclic series, which has *n*-Pr alkyl substituent like cyclopropyl, also improved LE value from compound **5** to reach the same level of LE with

compound **7**.

2.5. Chemistry

Compounds **4**–**7** were synthesized as shown in Scheme 1. After protecting NH moiety of 7-bromo isatin **19** with PMB, the Wolff–Kishner reduction gave lactam **21**. Methylation of **21** with methyl iodide produced the key intermediate **22**. Palladium-catalyzed boration of **22** with vinyl pinacol diborane gave **23**. **23** was hydrogenated with palladium hydroxide on carbon, and subsequent PMB deprotection gave compound **4**. PMB deprotection of **22** followed by palladium-catalyzed boration afforded compound **5**. Palladium catalyzed carbonylation of **22** gave **27**, and subsequent Curtius rearrangement produced the Boc-protected **28**. Deprotection of PMB and Boc with HBr-AcOH produced compound **6**, and **7** was prepared in the same procedure after methylation.

Compounds **8**–**10** were synthesized as shown in Scheme 2. The palladium-catalyzed Suzuki-Miyaura cross-coupling reaction of 2-bromoaniline **30** with cyclopropylboronic acid gave the cyclopropylbenzene **31**, and conversion of the amino group to the iodine via the Sandmeyer reaction provided the iodobenzene **32**. The palladium-mediated Buchwald-Hartwig type amination of the iodobenzene **32** and the aminopyridine **33** gave the compound **35**, and the subsequent intramolecular Heck-type cyclization provided the pyridoindole **8**. Pyridoindole **9** was prepared by the same procedure from **32** and **34**. The synthesis of compound **10** was started from 1-bromo-3-fluoro-2-nitrobenzene **37**. The fluorine in compound **38**, which was prepared from **37** and cyclopropylboronic acid by conducting the Suzuki-Miyaura cross-coupling reaction, was substituted by ethyl cyanoacetate to obtain **39**. Iron-mediated reduction of the nitro group in **39** was accompanied with direct cyclization and gave the indole **40**. The reaction of **40** and acetonitrile, treated under acidic conditions of 4*N*-HCl/dioxane first, then under basic conditions of saturated $NaHCO_3$ solution, gave the pyrimidoindole intermediate **41**. The hydroxyl group in **41** was converted to the chlorine **42** by treating with thionyl chloride, and subsequent hydrogenation with palladium hydroxide on carbon gave pyrimidoindole **10**.

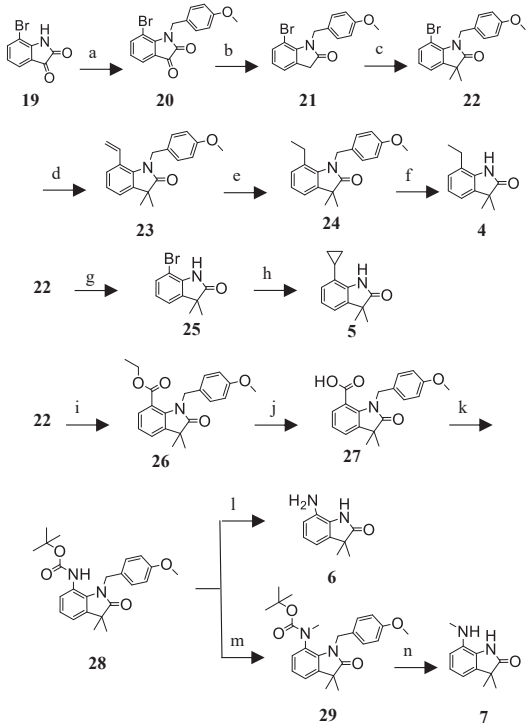

Scheme 1.

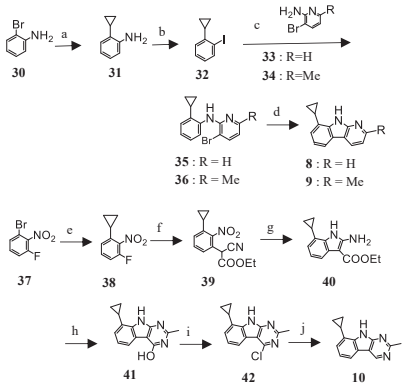

Scheme 2.

Compounds **11**–**15** were synthesized as shown in Scheme 3. For the synthesis of **11**, 4-chloro-2-methyl-7*H*-pyrrolo[2,3-*d*]pyrimidine **43** was protected by SEM to give **44**. Next, the 6-position of pyrrolopyrimidine was propylated and converted into **45**, and the chloro was removed reductively to obtain **46**. **46** was brominated with NBS to give 5-bromo compound **47**. Finally, cyanation of **47** and deprotection of SEM of **48** with BF_3-Et_2O yielded **11**. In the synthesis of **12** and **13**, compound **50** was synthesized by the Sonogashira reaction of 5-iodo-2-methylpyrimidin-4-amine **49** with 1-penthyne, and then pyrrole cyclization under basic conditions gave **51**. NCS-Chlorination and NBS-bromination of **51** gave **12** and **13,** respectively. The synthesis of **14** and **15** was started from **45** and bromination at the 5-position led to **52**. Conversion of the bromo of **52** to a methyl and then removal of SEM of **53** using TFA gave compound **15**. Subsequent reductive dehalogenation of chlorine gave **14**.

Compounds **16**–**18** were synthesized as shown in Scheme 4. Methylamide **16** was synthesized from 4-chloro-2-methyl-7*H*-pyrrolo[2,3-*d*]pyrimidine **43**. Similar to the synthesis of **53**, compound **43** was brominated to **54** and subsequently methylated to **55**. After Ts protection of the pyrrole nitrogen, introduction of the ethyl ester to the 6-position of **56** by anion reaction with ethyl carbonochloridate and *n*-BuLi gave compound **57**. After hydrolysis of the ester and deprotection of Ts with lithium hydroxide at the same time, to obtain carboxylic acid **58** was obtained. Methylamine, WSC, and DMAP were used to give methylamide **16**. Compounds **17** and **18** were both synthesized from **59** obtained by formylation of **44**. The Wittig reaction of the aldehyde **59** yielded *trans*-butene **60**, which was converted to **18** by SEM deprotection and NCS-chlorination. Carboxylic acid intermediate **62** was obtained from aldehyde **59** by the Pinnick oxidation. Subsequent amidation of **62** gave methyl amide **63**. NBS-Bromination gave 5-bromo

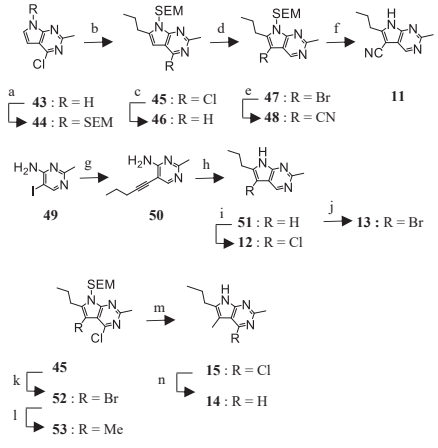

Scheme 3.

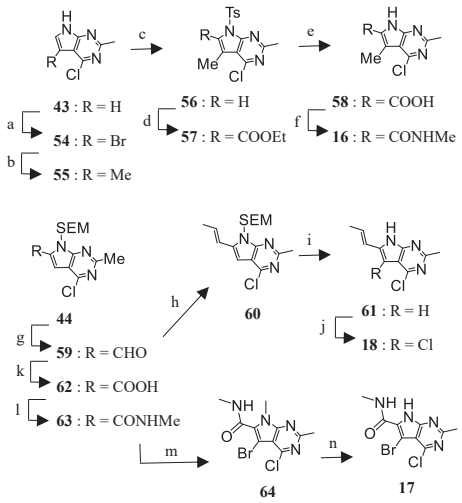

Scheme 4.

compound **64** and SEM removal gave compound **17**.

3. Conclusions

Three lead compounds with novel chemotypes that bound to the ATP binding site of PDHKs were successfully discovered by a fragment-based drug discovery approach. X-ray fragment screening toward PDHK4 was carried out to find ligands with novel chemotypes, and fragment **1** with the characteristic interaction in a deep pocket was selected for further optimization. Fragment hit **1** was bound more deeply in the binding pocket than the preceding inhibitors, and the analysis of the X-ray structure with WaterMap calculations provided the strategy to displace a remaining water molecule with a hydrophobic group. This strategy led to the discovery of compound **7** with a significant improvement in inhibition potency. Compound **7** showed IC_{50} values in low micromolar range against all PDHK isozymes with high ligand efficiency, and the X-ray structure of this compound with PDHK4 confirmed our design strategy. All three conserved water molecules in the deep pocket were displaced, and a hydrophobic group occupied the pocket interior. Compound **7** was selected as the first lead compound, and the selectivity profile was evaluated. The compound **7** showed little inhibition on HSP90 and BCKDK in the same GHKL family proteins, and showed decent selectivity profile in the kinase panel assay. To generate new lead compounds, we designed a tri-cyclic core as a potential new scaffold by superposing the binding pose of another fragment hit **2** with that of compound **7**. This merging strategy led to identifying a second lead compound **10** with a tri-cyclic core. SAR information was successfully transferred into the original fragment **2** bi-cyclic core giving the third lead compound **13**. The characteristic interaction of these novel inhibitors in a deep pocket provides new structural insights into the PDHKs ATP binding site and opens a novel direction for the development of more PDHKs inhibitors.

4. Experimental section

4.1. Chemistry

Solvents and reagents were obtained from commercial suppliers and used as received. Flash column chromatography was performed using Merck 230–400 mesh silica gel 60. Proton nuclear magnetic resonance (1H NMR) spectra were recorded on a Varian MERCURYplus-AS400, JEOL RESONANCE Inc. JNM-AL400, Bruker BioSpin K.K. AV400 or AVANCE III 400, or Agilent Technologies Inc. 400-MR spectrometer in the indicated solvent. Chemical shifts (δ) are reported in parts per million relative to internal standard tetramethylsilane. High-resolution mass spectra (HRMS) analyses were performed on an LC-MS system composed of Agilent 1290 Infinity LC and Thermo Fisher Orbitrap ID-X.

4.1.1. Preparation of compound 1,2, and 3

1,**2**, and **3** were obtained from commercial suppliers and used without further purification.

4.1.2. Synthesis of compound 4

Step 1: 7-Bromo-1-(4-methoxybenzyl)indoline-2,3-dione (**20**)

7-Bromo isatin (**19**; 2.5 g, 11.1 mmol) in DMF (10 mL) was added by drops, using a dropping funnel, into a solution of 60% sodium hydride (66 8 mg, 16.7 mmol) in DMF (20 mL) at 0 °C. *Para*- Methoxy benzyl chloride (2.3 mL, 16.7 mmol) was added dropwise at 0 °C, and the mixture was stirred at room temperature for 1.5 h. The reaction mixture was quenched with methanol (2 mL) at 0 °C and was diluted with H_2O and EtOAc. The organic layer was washed with H_2O and brine, and dried over Na_2SO_4. After filtration and concentration, the residue was purified by flash chromatography (solvent: EtOAc/$CHCl_3$ = 1/30 to 1/20) to give the title compound **20** (1.75 g, 46% yield).

^{1}H NMR (400 MHz, $CDCl_3$) δ: 3.78 (s, 3H), 5.38 (s, 2H), 6.86 (d, J = 8.8 Hz, 2H), 6.99 (dd, J = 8.0, 7.2 Hz, 1H), 7.23 (d, J = 8.8 Hz, 2H), 7.61 (dd, J = 7.2, 1.2 Hz, 1H), 7.67 (dd, J = 8.0, 1.2 Hz, 1H)

Step 2: 7-Bromo-1-(4-methoxybenzyl)indolin-2-one (**21**)

Hydrazine monohydrate (2 mL) was added to **20** (1.75 g, 5.06 mmol) in EtOH (20 mL) and stirred at 95 °C for 12 h. After cooling to room temperature, H_2O and EtOAc were added to the reaction mixture. The organic layer was washed with H_2O and brine, and dried over Na_2SO_4. After filtration and concentration, the residue was purified by flash chromatography (solvent: EtOAc/Hexane = 1/5, 1/4 to 1/3) to give the title compound **21** (876 mg, 52% yield).

^{1}H NMR (400 MHz, $CDCl_3$) δ: 3.77 (s, 3H), 5.34 (s, 2H), 6.84 (d, J = 8.8 Hz, 2H), 6.86–6.92 (m, 2H), 7.16–7.21 (m, 3H), 7.28–7.32 (m, 1H), 7.35 (dd, J = 8.4, 1.2 Hz, 1H)

Step 3: 7-Bromo-1-(4-methoxybenzyl)-3,3-dimethylindolin-2-one (**22**)

Compound **21** (876 mg, 2.64 mmol) in DMF (6 mL) was dropped into the solution of 60% sodium hydride (232 mg, 5.81 mmol) in DMF (6 mL) at 0 °C. Methyl iodide (489 μL, 7.92 mmol) was added dropwise, and the mixture was stirred at room temperature for 2 h. The reaction mixture was quenched with water at 0 °C, and extracted with EtOAc. The organic layer was washed with H_2O and brine, and dried over Na_2SO_4. After filtration and concentration, the residue was purified by flash chromatography (solvent: EtOAc/Hexane = 1/6 to 1/5) to give the title compound **22** (889 mg, 93% yield).

^{1}H NMR (400 MHz, $CDCl_3$) δ: 1.42 (s, 6H), 3.77 (s, 3H), 5.34 (s, 2H), 6.83 (d, J = 8.8 Hz, 2H), 6.90 (dd, J = 8.4, 7.2 Hz, 1H), 7.12–7.16 (m, 3H), 7.31 (dd, J = 8.4, 1.2 Hz, 1H)

Step 4: 1-(4-methoxybenzyl)-3,3-dimethyl-7-vinylindolin-2-one (**23**)

A mixture of **22** (100 mg, 0.28 mmol), vinyl pinacol diborane (71 μL, 0.42 mmol) and Na_2CO_3 (89.0 mg, 0.84 mmol) in DME (2 mL) and H_2O (1 mL) was treated with $PdCl_2$(dppf)-CH_2Cl_2 (11.0 mg, 0.014 mmol) and stirred at 95 °C for 3 h. After cooling to room temperature, H_2O and EtOAc were added to the reaction mixture. The organic layer was washed with H_2O and brine, and dried over Na_2SO_4. After filtration and concentration, the residue was purified by flash chromatography (solvent: EtOAc/Hexane = 1/5) to give the title compound **23** (80.0 mg, 93% yield).

^{1}H NMR (400 MHz, $CDCl_3$) δ: 1.44 (s, 6H), 3.78 (s, 3H), 5.08 (s, 2H), 5.20 (dd, J = 10.8, 1.2 Hz, 1H),5.48 (dd, J = 17.2, 1.2 Hz, 1H), 6.81–6.88 (m, 3H), 7.03 (dd, J = 7.6, 7.6 Hz, 1H), 7.09 (d, J = 8.8 Hz, 2H), 7.15–7.18 (m, 2H)

Step 5: 7-Ethyl-1-(4-methoxybenzyl)-3,3-dimethylindolin-2-one (**24**)

To a solution of **23** (80.0 mg, 0.26 mmol) in MeOH (3 mL) was added $Pd(OH)_2$ (10 mg) and stirred under 1.0 atm of hydrogen at room temperature for 12 h. After removal of the catalyst by Celite® filtration, the

filtrate was evaporated *in vacuo* to give the title compound **24** (73.0 mg, 91% yield).

^{1}H NMR (400 MHz, $CDCl_3$) δ: 1.10 (t, J = 7.6 Hz, 3H), 1.44 (s, 6H), 2.39 (q, J = 7.6 Hz, 2H), 3.77 (s, 3H), 5.10 (s, 2H), 6.83 (d, J = 8.8 Hz, 1H), 6.99–7.01 (m, 2H), 7.04 (d, J = 8.8 Hz, 2H), 7.10 (dd, J = 6.2, 2.2 Hz, 1H)

Step 6: 7-Ethyl-3,3-dimethylindolin-2-one (**4**)

TFA (2 mL) was added to **24** (73.0 mg, 0.24 mmol) and stirred at 60 °C for 2 h. The reaction mixture was evaporated *in vacuo* and quenched with saturated aqueous $NaHCO_3$. EtOAc was added, and the organic layer was separated. The organic layer was washed with H_2O and brine, and dried over Na_2SO_4. After filtration and concentration, the residue was purified by preparative TLC (solvent: EtOAc/Hexane = 1/3) to give the title compound **4** (28.0 mg, 62% yield).

^{1}H NMR (400 MHz, $CDCl_3$) δ: 1.26 (t, J = 7.6 Hz, 3H), 1.40 (s, 6H), 2.60 (q, J = 7.6 Hz, 2H), 6.98–7.07 (m, 3H), 7.91 (brs, 1H)

HRMS (ESI, *m/z*) calced for $C_{12}H_{14}ON$ $(M-H)^-$ 188.1081, found 188.1082

4.1.3. Synthesis of compound 5

Step 1: 7-Bromo-3,3-dimethylindolin-2-one (**25**)

TFA (2 mL) was added to **22** (310 mg, 0.86 mmol) and stirred at 50 °C for 2 h. The reaction mixture was evaporated *in vacuo* and quenched with saturated aqueous $NaHCO_3$. EtOAc was added, and the organic layer was separated. The organic layer was washed with H_2O and brine, and dried over Na_2SO_4. After filtration and concentration, the residue was purified by preparative TLC (solvent: EtOAc/$CHCl_3$ = 1/10) to give the title compound **25** (155 mg, 75% yield).

^{1}H NMR (400 MHz, $CDCl_3$) δ: 1.39 (s, 6H), 6.92 (dd, J = 8.2, 7.2 Hz, 1H), 7.10 (dd, J = 7.2, 1.0 Hz, 1H), 7.31 (dd, J = 8.2, 1.0 Hz), 7.47 (brs, 1H)

Step 2: 7-Cyclopropyl-3,3-dimethylindolin-2-one (**5**)

A mixture of **25** (80.0 mg, 0.33 mmol), cyclopropyl boronic acid (43.0 mg, 0.50 mmol) and Na_2CO_3 (140 mg, 1.32 mmol) in DME (3 mL) and H_2O (1 mL) was treated with $PdCl_2$(dppf)-CH_2Cl_2 (24.0 mg, 0.03 mmol) and stirred at 95 °C for 7 h. After cooling to room temperature, H_2O and EtOAc were added to the reaction mixture. The organic layer was washed with H_2O and brine, and dried over Na_2SO_4. After filtration and concentration, the residue was purified by preparative TLC (solvent: EtOAc/Hexane = 1/2) to give the title compound **5** (18.0 mg, 27% yield).

^{1}H NMR (400 MHz, $CDCl_3$) δ: 0.61–0.73 (m, 2H), 0.88–1.00 (m, 2H), 1.40 (s, 6H), 1.73–1.80 (m, 1H), 6.95–7.04 (m, 3H), 7.75 (brs, 1H)

HRMS (ESI, *m/z*) calced for $C_{13}H_{14}ON$ $(M-H)^-$ 200.1081, found 200.1081

4.1.4. Synthesis of compound 6

Step 1: Ethyl 1-(4-methoxybenzyl)-3,3-dimethyl-2-oxoindoline-7-carboxylate (**26**)

To a solution of **22** (400 mg, 1.11 mmol) in EtOH (10 mL) was added $PdCl_2$(dppf)-CH_2Cl_2 (180 mg, 0.22 mmol) and Et_3N (1.5 mL, 11.1 mmol), and stirred under 1.0 atm of carbon monoxide at 80 °C for 12 h. After cooling to room temperature, H_2O and EtOAc were added to the reaction mixture. The organic layer was washed with H_2O and brine, and dried over Na_2SO_4. After filtration and concentration, the residue was purified by flash chromatography (solvent: EtOAc/Hexane = 1/6 to 1/4) to give the title compound **26** (374 mg, 95% yield).

^{1}H NMR (400 MHz, $CDCl_3$) δ: 1.20 (t, J = 7.2 Hz, 3H), 1.45 (s, 6H), 3.73 (s, 3H), 4.14 (q, J = 7.2 Hz, 2H), 5.22 (s, 2H), 6.75 (d, J = 8.8 Hz, 2H), 6.92 (d, J = 8.8 Hz, 2H), 7.02 (dd, J = 7.8, 7.2 Hz, 1H), 7.32 (dd, J = 7.2, 1.4 Hz, 1H), 7.35 (dd, J = 7.8, 1.4 Hz, 1H)

Step 2: 1-(4-Methoxybenzyl)-3,3-dimethyl-2-oxoindoline-7-carboxylic acid (**27**)

To a solution of **26** (374 mg, 1.06 mmol) in MeOH (4 mL) and THF (2 mL) was added aqueous 2 N NaOH (1.1 mL, 2.12 mmol) at room temperature. The reaction mixture was stirred at 60 °C for 2 h. After cooling to 0 °C, aqueous 2 N HCl (1.1 mL, 2.12 mmol) was added. After evaporating *in vacuo*, H_2O and $CHCl_3$ were added to the residue. The organic layer was washed with H_2O and brine, and dried over Na_2SO_4. After filtration, the solvent was evaporated *in vacuo* to give the title compound **27** (360 mg, overweight) as a crude product. This was used in the next step without further purification.

^{1}H NMR (400 MHz, $CDCl_3$) δ: 1.47 (s, 6H), 3.71 (s, 3H), 5.28 (s, 2H), 6.73 (d, J = 8.6 Hz, 2H), 6.95 (d, J = 8.6 Hz, 2H), 7.08 (dd, J = 8.0, 7.2 Hz, 1H), 7.38 (dd, J = 7.2, 1.2 Hz, 1H), 7.56 (dd, J = 8.0, 1.2 Hz, 1H)

Step 3: *tert*-Butyl (1-(4-methoxybenzyl)-3,3-dimethyl-2-oxoindolin-7-yl)carbamate (**28**)

To a solution of **27** (360 mg, approx.1.06 mmol) in toluene (5 mL) were added Et_3N (233 μL, 1.67 mmol) and DPPA (310 μL, 1.44 mmol) and stirred at 85 °C for 10 min. *t*BuOH (1 mL) was added at room temperature and stirred at 60 °C for 3 h. After cooling to room temperature, H_2O and EtOAc were added to the reaction mixture. The organic layer was washed with H_2O and brine, and dried over Na_2SO_4. After filtration and concentration, the residue was purified by flash chromatography (solvent: EtOAc/Hexane = 1/6 to 1/4) to give the title compound **28** (290 mg, 19% yield for 2 steps).

^{1}H NMR (400 MHz, $CDCl_3$) δ: 1.47 (s, 6H), 1.50 (s, 9H), 3.78 (s, 3H), 5.04 (s, 2H), 6.87 (d, J = 8.8 Hz, 2H), 6.99–7.08 (m, 2H), 7.13–7.18 (m, 3H)

Step 4: 7-Amino-3,3-dimethylindolin-2-one (**6**)

HBr-AcOH (1 mL) was added to **28** (50.0 mg, 0.169 mmol) and stirred at r.t. for 16 h. After cooling to 0 °C, the reactant mixture was diluted with sat. aqueous $NaHCO_3$, and extracted with AcOEt. The organic layer was washed with H_2O and brine, dried over Na_2SO_4. After filtration and concentration, the residue was purified by preparative TLC (solvent: EtOAc/$CHCl_3$ = 1/1) to give the title compound **6** (4.0 mg, 13% yield).

^{1}H NMR (400 MHz, $CDCl_3$) δ: 1.38 (s, 6H), 6.63 (dd, J = 8.2, 1.4 Hz, 1H), 6.68 (dd, J = 7.2, 1.4 Hz), 6.90 (dd, J = 8.2, 7.2 Hz, 1H), 9.81 (brs, 1H)

HRMS (ESI, *m/z*) calced for $C_{10}H_{11}ON_2$ $(M-H)^-$ 175.0877, found 175.0878

4.1.5. Synthesis of compound 7

Step 1: *tert*-Butyl (1-(4-methoxybenzyl)-3,3-dimethyl-2-oxoindolin-7-yl)(methyl)carbamate (**29**)

28 (145 mg, 0.37 mmol) in DMF (2 mL) was dropped into a solution of 60% sodium hydride (18.0 mg, 0.44 mmol) in DMF (1 mL) at 0 °C. Methyl iodide (35.0 μL, 0.56 mmol) was added dropwise at 0 °C, and the mixture was stirred at room temperature for 3 h·H_2O and AcOEt were added to the reaction mixture, and the organic layer was separated. The organic layer was washed with H_2O and brine, dried over Na_2SO_4. After filtration, the solvent was evaporated *in vacuo* to give the title compound **29** (172 mg, overweight) as a crude product. This was used in the next step without further purification.

Step 2: 3,3-Dimethyl-7-(methylamino)indolin-2-one (**7**)

TFA (2 mL) was added to **29** (172 mg, approx. 0.37 mmol) in $CHCl_3$ (0.5 mL) and stirred at 80 °C for 24 h. The reaction mixture was evaporated *in vacuo* and quenched with saturated aqueous $NaHCO_3$. $CHCl_3$ was added, and the organic layer was separated. The organic layer was washed with H_2O and brine, dried over Na_2SO_4. After filtration and concentration, the residue was purified by preparative TLC (solvent: EtOAc/$CHCl_3$ = 1/5) to give the title compound **7** (50.0 mg, 70% yield for 2 steps).

^{1}H NMR (400 MHz, $CDCl_3$) δ: 1.38 (s, 6H), 2.92 (s, 3H), 3.94 (brs, 1H), 6.59 (d, J = 8.0 Hz, 1H), 6.64 (d, J = 7.2 Hz, 1H), 7.00 (dd, J = 8.0, 7.2 Hz, 1H)

HRMS (ESI, *m/z*) calced for $C_{11}H_{15}ON_2$ $(M+H)^+$ 191.1179, found 191.1175

4.1.6. Synthesis of compound 8

Step 1: 2-Cyclopropylaniline (**31**)

A mixture of 2-bromoaniline (**30**; 32.0 g, 186 mmol), cyclopropylboronic acid (23.9 g, 278 mmol), and K_3PO_4 (113 g, 532 mmol) in toluene (350 mL) and H_2O (100 mL) was treated with $PdCl_2$(dppf)-CH_2Cl_2 (5.66 g, 6.93 mmol) and stirred at 90 °C for 5 h under argon atmosphere. The mixture was cooled to 0 °C, ammonium pyrrolidinedithiocarbamate (APDTC, 5.06 g, 30.8 mmol) was added and the mixture was stirred at room temperature for 1 h. The reactant mixture was filtered through Celite®, and the organic layer was separated and washed with H_2O and brine. The resultant organic layer was loaded on silica gel column chromatography (eluted with *n*-hexane/EtOAc = 80/20 (v/v), approximately 1.6 L) for elimination of the polar component. The eluate was acidified by adding 4 M HCl in AcOEt (50 mL) without concentration. The precipitated crystals were collected by filtration, washed with EtOAc and *n*-hexane, and dried to give the hydrochloride salt of the title compound **31** as a white crystalline (28.6 g, 90% yield).

^{1}H NMR (400 MHz, DMSO-d_6) δ: 0.69–0.73 (m, 2H), 0.95–1.00 (m, 2H), 1.97–2.06 (br m, 1H), 7.09–7.05 (m, 1H), 7.22–7.26 (m, 1H), 7.31–7.39 (br m, 1H), 9.90 (br s, 3H).

Step 2: 1-Cyclopropyl-2-iodobenzene (**32**)

Sodium nitrate (11.5 g, 167 mmol) in H_2O (70 mL) was dropped into the mixture of the hydrochloride salt of **31** (25.6 g, 151 mmol) and 1 M aqueous HCl solution (20 mL) at 0 °C. After stirring at 0 °C for 15 min, to the reaction mixture was added sodium iodide (24.9 g, 166 mmol) in H_2O (70 mL) at 0 °C. The mixture was stirred at 0 °C for 30 min and then room temperature for 2 h. The reactant mixture was quenched with aqueous NaS_2O_3, and the mixture was extracted with EtOAc. The extract was washed with H_2O and brine, and dried over Na_2SO_4. The solvent was evaporated *in vacuo*. The residue was purified by flash chromatography (Biotage-SNAP Ultra 100 g, eluted with *n*-hexane/EtOAc = 100/0 to 95/5 (v/v)) to give the title compound **32** (31.9 g, 86% yield).

^{1}H NMR (400 MHz, $CDCl_3$) δ: 0.63–0.68 (m, 2H), 0.99–1.05 (m, 2H), 1.98–2.06 (m, 1H), 6.88 (t, J = 7.7 Hz, 1H), 6.92 (d, J = 7.7 Hz, 1H), 7.24 (t, J = 7.7 Hz, 1H), 7.83 (d, J = 7.7 Hz, 1H)

Step 3: 3-Bromo-*N*-(2-cyclopropylphenyl)pyridin-2-amine (**35**)

A mixture of **32** (1.00 g, 4.10 mmol), 3-bromopyridin-2-amine (**33**; 709 mg, 4.10 mmol), and sodium *tert*-pentoxide (902 mg, 8.19 mmol) in toluene (10 mL) was treated with $Pd(OAc)_2$ (92.0 mg, 0.41 mmol) and Xantphos (237 mg, 0.41 mmol) and stirred at 140 °C for 4.5 h under argon atmosphere. After cooling to room temperature, the mixture was diluted with EtOAc and H_2O. The insoluble solid was filtered through Celite®. The organic layer was separated from the filtrate and concentrated. The residue was purified by flash chromatography (Biotage-SNAP Ultra 25 g, eluted with *n*-hexane/EtOAc = 99/1 to 90/10 (v/v)) to give the title compound **35** (945 mg, 80% yield).

^{1}H NMR (400 MHz, $CDCl_3$) δ: 0.67–0.78 (m, 2H), 0.97–1.12 (m, 2H), 1.80–1.91 (m, 1H), 6.63 (dd, J = 7.7, 4.9 Hz, 1H), 6.97 (td, J = 7.7, 1.2 Hz, 1H), 7.19 (dt, J = 7.7, 1.2 Hz, 1H), 7.26 (td, J = 8.1, 1.2 Hz, 1H), 7.75 (dd, J = 7.7, 1.6 Hz, 1H), 7.78 (br s, 1H), 8.18 (dd, J = 4.9, 1.6 Hz, 1H), 8.39 (dd, J = 8.1, 1.2 Hz, 1H)

Step 4: 8-Cyclopropyl-9*H*-pyrido[2,3-*b*]indole (**8**)

A solution of **35** (945 mg, 3.27 mmol) and DBU (1.48 mL, 9.80 mmol) in DMA (19 mL) was treated with $Pd(OAc)_2$ (73.4 mg, 0.327 mmol) and CyJohnPhos (229 mg, 0.65 mmol) under argon atmosphere and stirred at 140 °C for 2 h. After cooling to room temperature, the mixture was diluted with H_2O and extracted with EtOAc. The organic layer was washed twice with H_2O and brine, and dried over Na_2SO_4. After filtration and concentration, the residue was purified by flash chromatography (Biotage-SNAP Ultra 25 g, eluted with *n*-hexane/EtOAc = 92/8 to 34/66 (v/v)). After concentration, for further purification, the residue was slurried in *n*-hexane/AcOEt (2/1 (v/v)). The precipitated solid was collected by filtration, washed with *n*-hexane, and dried to give the title compound **8** (251 mg, 37% yield).

^{1}H NMR (400 MHz, DMSO-d_6) δ: 0.76–0.80 (m, 2H), 1.03–1.08 (m, 2H), 2.38–2.45 (m, 1H), 6.99 (d, J = 7.6 Hz, 1H), 7.13 (t, J = 7.6 Hz, 1H), 7.20 (dd, J = 7.8, 4.8 Hz, 1H), 7.95 (d, J = 7.6 Hz, 1H), 8.43 (dd, J = 4.8, 1.5 Hz, 1H), 8.48 (dd, J = 7.8, 1.5 Hz, 1H), 11.92 (s, 1H)

HRMS (ESI, *m/z*) calced for $C_{14}H_{13}N_2$ $(M + H)^+$ 209.1073, found 209.1072

4.1.7. Synthesis of compound 9

Step 1: 3-Bromo-*N*-(2-cyclopropylphenyl)-6-methylpyridin-2-amine (**36**)

A mixture of **32** (150 mg, 0.615 mmol), 3-bromo-6-methylpyridin-2-amine (**34**; 138 mg, 0.738 mmol), and cesium carbonate (300 mg, 0.921 mmol) in toluene (1.5 mL) was treated with $Pd(OAc)_2$ (28.0 mg, 0.125 mmol) and Xantphos (72.0 mg, 0.139 mmol) and stirred at 130 °C for 3 h under argon atmosphere. After cooling to room temperature, the mixture was diluted with EtOAc and H_2O. The insoluble solid was filtered through Celite®. The organic layer was separated from the filtrate and concentrated. The residue was purified by flash chromatography (Biotage-SNAP Ultra 10 g, eluted with *n*-hexane/EtOAc = 99/2 to 85/25 (v/v)) to give the title compound **36** (64.0 g, 34% yield).

^{1}H NMR (400 MHz, $CDCl_3$) δ: 0.70–0.75 (m, 2H), 1.03–1.09 (m, 2H), 1.80–1.89 (m, 1H), 2.45 (s, 3H), 6.51 (d, J = 7.9 Hz, 1H), 6.94 (td, J = 7.6, 1.3 Hz, 1H), 7.19 (dt, J = 7.6, 1.3 Hz, 1H), 7.25 (td, J = 8.1, 1.3 Hz, 1H), 7.62 (d, J = 7.9 Hz, 1H), 7.82 (s, 1H), 8.58 (dd, J = 8.1, 1.3 Hz, 1H)

Step 2: 8-Cyclopropyl-2-methyl-9*H*-pyrido[2,3-*b*]indole (**9**)

A solution of **36** (64 mg, 0.211 mmol) and DBU (63.0 μL, 0.421 mmol) in DMA (1.0 mL) was treated with $Pd(OAc)_2$ (14.0 mg, 6.24 × 10v mmol) and CyJohnPhos (22.0 mg, 6.28×10^{-2} mmol) under argon atmosphere and stirred at 140 °C for 20 h. After cooling to room temperature, the mixture was diluted with H_2O and extracted with EtOAc. The organic layer was washed twice with H_2O and brine, and dried over Na_2SO_4. After filtration and concentration, the residue was purified by flash chromatography (Biotage-SNAP Ultra 10 g, eluted with *n*-hexane/EtOAc = 90/10 to 0/100 (v/v)). After concentration, for further purification, the residue was purified by preparative TLC (*n*-hexane/AcOEt = 1/1 (v/v)) to give the title compound **9** (35 mg, 75% yield).

^{1}H NMR (400 MHz, $CDCl_3$) δ: 0.77–0.81 (m, 2H), 1.01–1.05 (m, 2H), 2.06–2.14 (m, 1H), 2.69 (s, 3H), 7.05 (d, J = 7.8 Hz, 1H), 7.16–7.22 (m, 2H), 7.85 (dd, J = 7.2, 1.8 Hz, 1H), 8.19 (d, J = 7.8 Hz, 1H), 8.67 (s, 1H)

HRMS (ESI, *m/z*) calced for $C_{15}H_{15}N_2$ $(M + H)^+$ 223.1230, found 223.1226

4.1.8. Synthesis of compound 10

Step 1: 1-Cyclopropyl-3-fluoro-2-nitrobenzene (**38**)

A mixture of 1-bromo-3-fluoro-2-nitrobenzene (**37**, 49.8 g, 226 mmol), cyclopropylboronic acid (21.4 g, 249 mmol), and K_3PO_4 (106 g, 499 mmol) in DME (300 mL) and H_2O (150 mL) was treated with $PdCl_2$(dppf)-CH_2Cl_2 (9.25 g, 11.3 mmol) and stirred under reflux for 1 h. After cooling to room temperature, the mixture was diluted with AcOEt and H_2O, filtered through Celite®, and the organic layer was separated and washed with H_2O and brine. After filtration and concentration, the residue was purified by flash chromatography (solvent: EtOAc/Hexane = 5/95 to 25/75) to give the title compound **38** (36.8 g, 89% yield).

^{1}H NMR (400 MHz, DMSO-d_6) δ: 0.77–0.81 (m, 2H), 0.99–1.04 (m, 2H), 1.85–1.92 (m, 1H), 7.03–7.05 (m, 1H), 7.35–7.40 (m, 1H), 7.52–7.58 (m, 1H)

Step 2: Ethyl 2-cyano-2-(3-cyclopropyl-2-nitrophenyl)acetate (**39**)

Compound **38** (3.00 g, 16.6 mmol) and ethyl 2-cyanoacetate (3.50 mL, 33.1 mmol) was dissolved in DMF (15 mL). To the solution, K_2CO_3 (6.90 g, 49.7 mmol) was added, and the mixture was stirred at 90 °C for 3 h. After cooling to 0 °C, the reactant mixture was diluted with H_2O (50 mL), acidified by adding 6.0 M aqueous HCl solution (25 mL), and extracted with 1:1n-hexane-AcOEt. The organic layer was washed with H_2O and brine, and dried over Na_2SO_4. After filtration, the solvent was evaporated *in vacuo* to give the title compound **39** (5.0 g, overweight) as a crude product which was used for the next step without further purification.

^{1}H NMR (400 MHz, $CDCl_3$) δ: 0.64–0.77 (m, 2H), 0.96–1.06 (m, 2H), 1.30 (t, J = 7.3 Hz, 3H), 1.98–2.06 (m, 1H), 4.26 (q, J = 7.3 Hz, 2H), 5.00 (s, 1H), 7.21 (dd, J = 7.7, 0.8 Hz, 1H), 7.04 (t, J = 7.7 Hz, 1H), 7.54

(dd, J = 7.7,1.6 Hz, 1H)

Step 3: Ethyl 2-amino-7-cyclopropyl-1*H*-indole-3-carboxylate (**40**)

To the solution of **39** (5.0 g, approx. 16 mmol) in AcOH (30 mL) was added iron powder (5.09 g, 91.1 mmol), and the mixture was stirred at 90 °C for 2 h. After cooling to room temperature, the reactant mixture was diluted with 1:1 toluene-H_2O (60 mL), filtered through Celite®, and the organic layer was separated and washed with H_2O, saturated $NaHCO_3$ solution and brine sequentially, and dried over Na_2SO_4. After filtration and concentration, the residue was purified by flash chromatography (Yamazen-Universal Premium L, eluted with *n*-hexane/EtOAc = 85/15 to 40/60 (v/v)) to give the title compound **40** (2.10 g, 52% two-step yield from **38**).

^{1}H NMR (400 MHz, $CDCl_3$) δ: 0.71 (br s, 2H), 0.93 (br s, 2H), 1.42 (t, J = 7.1 Hz, 3H), 1.91 (br s, 1H), 4.36 (q, J = 7.1 Hz, 2H), 5.68 (br s, 1H), 6.79 (d, J = 7.4 Hz, 1H), 7.04 (t, J = 7.4 Hz, 1H), 7.64 (d, J = 7.4 Hz, 1H), 7.92 (br s, 2H)

Step 4: 8-Cyclopropyl-2-methyl-9*H*-pyrimido[4,5-*b*]indol-4-ol (**41**)

Compound **40** (5.00 g, 20.5 mmol) was dissolved in 4 M aqueous HCl solution (25 mL). To the solution, MeCN (7.5 mL) was added, and the mixture was stirred at room temperature for 20 h. The resultant suspension was diluted with 1:1*n*-hexane-dioxane (50 mL), and the precipitated solid was collected by filtration, washed with *n*-hexane, and dried *in vacuo*. The obtained solid was redissolved in MeOH (65 mL) and H_2O (20 mL). Saturated $NaHCO_3$ solution (40 mL) was added to the solution, and the reactant mixture was stirred at 75 °C for 2.5 h. After cooling to 0 °C, the reactant mixture was acidified by adding 6 M aqueous HCl solution (7.5 mL), diluted with H_2O (100 mL), and then stirred at 0 °C for 15 min. The precipitated solid was collected by filtration, washed with H_2O, and dried to give the title compound **41** (4.88 mg, 99% yield).

^{1}H NMR (400 MHz, DMSO-d_6) δ: 0.77–0.73 (m, 2H), 0.99–1.04 (m, 2H), 2.30–2.37 (m, 1H), 2.42 (s, 3H), 6.80 (d, J = 7.5 Hz, 1H), 7.10 (t, J = 7.5 Hz, 1H), 7.73 (dd, J = 7.5, 0.9 Hz, 1H), 12.07 (s, 1H), 12.12 (s, 1H)

Step 5: 4-Chloro-8-cyclopropyl-2-methyl-9*H*-pyrimido [4,5-b] indole (**42**)

To a suspension of **41** (4.88 g, 20.4 mmol) in $CHCl_3$ (66 mL) was added thionyl chloride (7.42 mL, 102 mmol) and DMF (33 mL), and the mixture was stirred at 60 °C for 2 h. The resultant solution was cooled to 0 °C and quenched with H_2O. The mixture was extracted with AcOEt, and the organic layer was washed twice with H_2O and brine, and dried over Na_2SO_4. After filtration and concentration, the residue was purified by flash chromatography (Yamazen-Universal Premium 3L, eluted with *n*-hexane/EtOAc = 90/10 to 20/80 (v/v)) to give the title compound **42** (2.44 mg, 46% yield).

^{1}H NMR (400 MHz, $CDCl_3$) δ: 2.05–2.09 (m, 2H), 2.27–2.31 (m, 2H), 3.08–3.14 (m, 1H), 3.68 (s, 3H), 7.26–7.31 (m, 2H), 7.93–7.98 (m, 1H), 8.84 (s, 1H)

Step 6: 8-Cyclopropyl-2-methyl-9*H*-pyrimido[4,5-*b*]indole (**10**)

A solution of **42** (40.0 mg, 0.155 mmol) in THF (0.6 mL) and MeOH (0.6 mL) was treated with 10% palladium hydroxide on activated carbon (15.0 mg) and K_2CO_3 (32.0 mg, 0.233 mmol), and the mixture was stirred under 1.0 atm of hydrogen at room temperature for 7 h. After removal of the palladium catalyst by Celite® filtration, the filtrate was concentrated. The residue was suspended in 1:1*n*-hexane-AcOEt and slurried for a while. The precipitated solid was collected by filtration, washed with 2:1*n*-hexane-AcOEt, and dried to give the title compound **10** (30.0 mg, 86% yield).

^{1}H NMR (400 MHz, DMSO-d_6) δ: 0.77–0.81 (m, 2H), 1.04–1.09 (m, 2H), 2.33–2.40 (m, 1H), 2.71 (s, 3H), 7.02 (d, J = 7.6 Hz, 1H), 7.20 (t, J = 7.6 Hz, 1H), 7.97 (d, J = 7.6 Hz, 1H), 9.30 (s, 1H), 12.27 (s, 1H).

HRMS (ESI, *m/z*) calced for $C_{14}H_{14}N_3$ $(M + H)^+$ 224.1182, found 224.1183

4.1.9. Synthesis of compound 11

Step 1: 4-Chloro-2-methyl-7-((2-(trimethylsilyl)ethoxy)methyl)-7*H*-pyrrolo[2,3-*d*]pyrimidine (**44**)

4-Chloro-2-methyl-7*H*-pyrrolo[2,3-*d*]pyrimidine (**43**, 5.00 g, 29.8 mmol) was added to a suspension of sodium hydride 60% dispersion in mineral oil (1.43 g, 35.8 mmol) and DMF (30 mL) at 0 °C. After stirring for 30 min at 0 °C, 2-(chloromethoxy)ethyltrimethylsilane (6.79 mL, 38.7 mmol) was added to the solution at 0 °C, and the mixture was stirred at room temperature for 1.5 h. The mixture was diluted with H_2O and extracted with EtOAc, and the organic layer was washed with H_2O and brine, and dried over $MgSO_4$. After filtration and concentration, the residue was purified by silica gel column chromatography (eluted with *n*-hexane/EtOAc = 100/0 to 90/10 (v/v)) to give the title compound **44** (7.80 g, 89% yield).

^{1}H NMR (400 MHz, DMSO-d_6) δ: −0.10 (s, 9H), 0.81–0.86 (m, 2H), 2.65 (s, 3H), 3.50–3.55 (m, 2H), 5.59 (s, 2H), 6.63 (d, J = 3.7 Hz, 1H), 7.75 (d, J = 3.7 Hz, 1H)

Step 2: 4-Chloro-2-methyl-6-propyl-7-((2-(trimethylsilyl)ethoxy)methyl)-7*H*-pyrrolo[2,3-*d*]pyrimidine (**45**)

To a solution of **44** (2.00 g, 6.71 mmol) in THF (20 mL), 1.63 M *n*-butyllithium in hexane (5.34 mL, 8.70 mmol) was added at −78 °C. After stirring for 3 h at −78 °C, 1-iodopropane (847 μL, 8.72 mmol) was added to the reactant mixture, and then the mixture was stirred at room temperature for 1.5 h. The mixture was diluted with H_2O and extracted with AcOEt, and the organic layer was washed with H_2O and brine, and dried over $MgSO_4$. After filtration and concentration, the residue was loaded on silica gel column chromatography (eluted with *n*-hexane/EtOAc = 100/0 to 95/5 (v/v)) for elimination of the polar component. The title compound **45** (1.10 g) was obtained as a mixture with unknown compounds, which was applied to the next step without further purification.

Step 3: 2-Methyl-6-propyl-7-((2-(trimethylsilyl)ethoxy)methyl)-7*H*-pyrrolo[2,3-*d*]pyrimidine (**46**)

A solution of **45** (1.10 g, ~3.2 mmol) and potassium carbonate (450 mg, 3.26 mmol) in MeOH (11 mL) was treated with 10% palladium on activated carbon (110 mg) and stirred under 1.0 atm of hydrogen overnight at room temperature. After removal of the palladium catalyst by Celite® filtration, the filtrate was diluted with H_2O and extracted with AcOEt. The organic layer was washed with H_2O and brine, and dried over $MgSO_4$. After filtration and concentration, the title compound **46** (1.00 g) was obtained, which was applied to the next step without further purification.

Step 4: 5-Bromo-2-methyl-6-propyl-7-((2-(trimethylsilyl)ethoxy)methyl)-7*H*-pyrrolo[2,3-*d*]pyrimidine (**47**)

To a solution of **46** (1.00 g, ~3.2 mmol) in DMF (20 mL) was added *N*-bromosuccinimide (582 mg, 3.27 mmol). After stirring at room temperature for 1 h, the reactant mixture was quenched with saturated $NaHCO_3$ solution. The mixture was extracted with AcOEt, and the organic layer was washed with H_2O and brine, and dried over $MgSO_4$. After filtration and concentration, the residue was purified by silica gel column chromatography (eluted with *n*-hexane/EtOAc = 95/5 to 90/10 (v/v)) to give the title compound **47** (770 mg, 30% yield, 3 steps from **44**).

^{1}H NMR (400 MHz, DMSO-d_6) δ: −0.10 (s, 9H), 0.82–0.87 (m, 2H), 0.95 (t, J = 7.6 Hz, 3H), 1.69 (tq, J = 7.6, 7.6 Hz, 2H), 2.67 (s, 3H), 2.84 (t, J = 7.6 Hz, 2H), 3.48–3.54 (m, 2H), 5.64 (s, 2H), 8.72 (d, 1H)

Step 5: 2-Methyl-6-propyl-7-((2-(trimethylsilyl)ethoxy)methyl)-7*H*-pyrrolo[2,3-*d*]pyrimidine-5-carbonitrile (**48**)

To a solution of **47** (200 mg, 0.520 mmol) in THF (2.0 mL), 1.63 M *n*-butyllithium in hexane (414 μL, 0.676 mmol) was added at −78 °C. After stirring for 1 h at −78 °C, *p*-toluenesulfonyl cyanide (122 mg, 0.673 mmol) was added to the reactant mixture, and then the mixture was stirred at room temperature for 3 h. The mixture was quenched with saturated NH_4Cl solution and extracted with AcOEt. The organic layer was washed with H_2O and brine, and dried over $MgSO_4$. After filtration and concentration, the residue was purified by preparative TLC (*n*-hexane/AcOEt = 4/1 (v/v)) to give the title compound **48** (110 mg) as a mixture with 2-methyl-6-propyl-7-((2-(trimethylsilyl)ethoxy)methyl)-7*H*-pyrrolo[2,3-*d*]pyrimidine, which was applied to the next step without further purification.

Step 6: 2-Methyl-6-propyl-7*H*-pyrrolo[2,3-*d*]pyrimidine-5-carbonitrile (**11**)

To a solution of **48** (50.0 mg, ~0.150 mmol) in CH_2Cl_2 (1.0 mL), boron trifluoride diethyl etherate (57.0 μL, 0.512 mmol) was added at room temperature. After stirring overnight at room temperature, the mixture was quenched with saturated $NaHCO_3$ solution and extracted with AcOEt. The organic layer was washed with H_2O and brine, and dried over $MgSO_4$. After filtration and concentration, for purification, the residue was slurried in *n*-hexane/AcOEt (1/1 (v/v)). The precipitated solid was collected by filtration, washed with *n*-hexane, and dried to give the title compound **11** (13.0 mg, 28% yield, 2 steps from **47**).

^{1}H NMR (400 MHz, DMSO-d_6) δ: 0.92 (t, J = 7.4 Hz, 3H), 1.77 (tq, J = 7.4, 7.4 Hz, 2H), 2.65 (s, 3H), 2.87 (t, J = 7.4 Hz, 2H), 8.93 (s, 1H), 12.89 (br s, 1H)

HRMS (ESI, *m/z*, MH+) Calcd for $C_{11}H_{13}N_4$: 201.1135, Found: 201.1138

4.1.10. Synthesis of compound 12

Step 1: 2-Methyl-5-(pent-1-yn-1-yl)pyrimidin-4-amine (**50**)

A solution of 5-iodo-2-methylpyrimidin-4-amine (**49**, 640 mg, 2.72 mmol), 1-penthyne (805 μL, 8.17 mmol), [1,1′-bis(diphenylphosphino) ferrocene]dichloropalladium(II) (220 mg, 0.269 mmol), copper(I) iodide (51.0 mg, 0.268 mmol) and triethylamine (569 μL, 4.08 mmol) in DMF (10 mL) was stirred at 70 °C for 2 h under argon atmosphere. The mixture was cooled to room temperature, diluted with H_2O and extracted with AcOEt. The organic layer was washed with H_2O and brine, and dried over $MgSO_4$. After filtration and concentration, the residue was loaded on silica gel column chromatography (eluted with *n*-hexane/EtOAc = 50/50 (v/v)) for elimination of the polar component. The title compound **50** (305 mg, 64% yield) was obtained, which was advanced to the next step without further purification.

Step 2: 2-Methyl-6-propyl-7*H*-pyrrolo[2,3-*d*]pyrimidine (**51**)

To a solution of **50** (300 mg, 1.71 mmol) in NMP (3.0 mL), potassium *tert*-butoxide (400 mg, 3.56 mmol) was added at room temperature and then stirred at 100 °C for 1 h. The mixture was cooled to room temperature, quenched with 1 N HCl solution and extracted with AcOEt. The organic layer was washed with H_2O and brine, and dried over $MgSO_4$. After filtration and concentration, the residue was purified by silica gel column chromatography (eluted with EtOAc) to give the title compound **51** (155 mg, 52% yield).

^{1}H NMR (400 MHz, DMSO-d_6) δ: 0.92 (t, J = 7.4 Hz, 3H), 1.70 (qt, J = 7.4, 7.4 Hz, 2H), 2.58 (s, 3H), 2.68 (t, J = 7.4 Hz, 2H), 6.19 (br s, 1H), 8.69 (s, 1H), 11.67 (br s, 1H)

Step 3: 5-Chloro-2-methyl-6-propyl-7*H*-pyrrolo[2,3-*d*]pyrimidine (**12**)

To a solution of **51** (30.0 mg, 0.171 mmol) in DMF (1.0 mL) was added *N*-chlorosuccinimide (34.0 mg, 0.255 mmol). After stirring at room temperature for 5 h, the reactant mixture was quenched with saturated $NaHCO_3$ solution. The mixture was extracted with AcOEt, and the organic layer was washed with H_2O and brine, and dried over $MgSO_4$. After filtration and concentration, the residue was purified by preparative TLC (*n*-hexane/AcOEt = 1/1 (v/v)) to give the title compound **12** (18.0 mg, 50% yield).

^{1}H NMR (400 MHz, DMSO-d_6) δ: 0.90 (t, J = 7.4 Hz, 3H), 1.69 (qt, J = 7.4, 7.4 Hz, 2H), 2.62 (s, 3H), 2.72 (t, J = 7.4 Hz, 2H), 8.73 (s, 1H), 12.11 (br s, 1H)

HRMS (ESI, *m/z*, MH+) Calcd for $C_{10}H_{13}N_3Cl$: 210.0793, Found: 210.0788

4.1.11. Synthesis of compound 13

To a solution of **51** (45.0 mg, 0.256 mmol) in $CHCl_3$ (1.0 mL) was added *N*-bromosuccinimide (55.0 mg, 0.308 mmol). After stirring overnight at room temperature, the reactant mixture was quenched with saturated $NaHCO_3$ solution. The mixture was extracted with AcOEt, and the organic layer was washed with H_2O and brine, and dried over $MgSO_4$. After filtration and concentration, for purification, the residue was slurried in *n*-hexane/AcOEt (2/1 (v/v)). The precipitated solid was collected by filtration, washed with *n*-hexane, and dried to give the title compound **13** (41.0 mg, 63% yield).

^{1}H NMR (400 MHz, DMSO-d_6) δ: 0.90 (t, J = 7.4 Hz, 3H), 1.69 (qt, J = 7.4, 7.4 Hz, 2H), 2.63 (s, 3H), 2.71 (t, J = 7.4 Hz, 2H), 8.65 (s, 1H), 12.23 (br s, 1H)

HRMS (ESI, *m/z*, MH+) Calcd for $C_{10}H_{13}N_3Br$: 254.0284, Found: 254.0287

4.1.12. Synthesis of compound 15

Step 1: 5-Bromo-4-chloro-2-methyl-6-propyl-7-((2-(trimethylsilyl) ethoxy)methyl)-7*H*-pyrrolo[2,3-*d*]pyrimidine (**52**)

To a solution of **45** (450 mg, 1.32 mmol) in DMF (5.0 mL) was added *N*-bromosuccinimide (260 mg, 1.46 mmol). After stirring overnight at room temperature, the reactant mixture was quenched with saturated $NaHCO_3$ solution. The mixture was extracted with AcOEt, and the organic layer was washed with H_2O and brine, and dried over $MgSO_4$. After filtration and concentration, the residue was loaded on silica gel column chromatography (eluted with *n*-hexane/EtOAc = 90/10 (v/v)) for elimination of the polar component. The title compound **52** (500 mg, 90% yield) was obtained, which was proceeded to the next step without further purification.

Step 2: 4-Chloro-2,5-dimethyl-6-propyl-7-((2-(trimethylsilyl)ethoxy) methyl)-7*H*-pyrrolo[2,3-*d*]pyrimidine (**53**)

To a solution of **52** (500 mg, 1.19 mmol) in THF (5.0 mL), 1.63 M *n*-butyllithium in hexane (950 μL, 1.55 mmol) was added at −78 °C. After stirring for 1 h at −78 °C, methyl iodide (96.0 μL, 1.54 mmol) was added to the reactant mixture, and then the mixture was stirred at room temperature for 2 h. The mixture was diluted with H_2O and extracted with AcOEt. The organic layer was washed with H_2O and brine, and dried over $MgSO_4$. After filtration and concentration, the residue was purified by silica gel column chromatography (eluted with *n*-hexane/EtOAc = 90/10 (v/v)) to give the title compound **53** (337 mg, 80% yield).

^{1}H NMR (400 MHz, DMSO-d_6) δ: −0.10 (s, 9H), 0.81–0.87 (m, 2H), 0.93 (t, J = 7.4 Hz, 3H), 1.61 (qt, J = 7.4, 7.4 Hz, 2H), 2.35 (s, 3H), 2.59 (s, 3H), 2.78 (t, J = 7.4 Hz, 2H), 3.45–3.50 (m, 2H), 5.58 (s, 2H)

Step 3: 4-Chloro-2,5-dimethyl-6-propyl-7*H*-pyrrolo[2,3-*d*]pyrimidine (**15**)

Compound **53** (150 mg, 0.424 mmol) was dissolved in TFA (1.5 mL), and the mixture was stirred at room temperature for 1 h. After evaporation of TFA, the residue was diluted with THF and neutralized with 2 N NaOH solution, and then extracted with AcOEt. The organic layer was washed with H_2O, 1 N HCl solution and brine, and dried over $MgSO_4$. After filtration and concentration, for purification, the residue was slurried in *n*-hexane/AcOEt (10/1 (v/v)). The precipitated solid was collected by filtration, washed with *n*-hexane, and dried to give the title compound **15** (35.0 mg, 37% yield).

^{1}H NMR (400 MHz, DMSO-d_6) δ: 0.88 (t, J = 7.4 Hz, 3H), 1.63 (qt, J = 7.4, 7.4 Hz, 2H), 2.31 (s, 3H), 2.55 (s, 3H), 2.65 (t, J = 7.4 Hz, 2H), 11.88 (br s, 1H)

HRMS (ESI, *m/z*, MH+) Calcd for $C_{11}H_{15}N_3Cl_1$: 224.0949, Found: 224.0950

4.1.13. Synthesis of compound 14

A solution of **15** (25.0 mg, 0.112 mmol) and potassium carbonate (15.0 mg, 0.109 mmol) in MeOH (1.0 mL) was treated with 10% palladium on activated carbon (10 mg) and stirred under 1.0 atm of hydrogen at room temperature for 2 h. After removal of the palladium catalyst by Celite® filtration, the filtrate was diluted with H_2O and extracted with AcOEt. The organic layer was washed with H_2O and brine, and dried over $MgSO_4$. After filtration and concentration, for purification, the residue was slurried in *n*-hexane/AcOEt (1/1 (v/v)). The precipitated solid was collected by filtration, washed with *n*-hexane, and dried to give the title compound **14** (17.0 mg, 81% yield).

^{1}H NMR (400 MHz, DMSO-d_6) δ: 0.88 (t, J = 7.4 Hz, 3H), 1.64 (qt, J = 7.4, 7.4 Hz, 2H), 2.18 (s, 3H), 2.57 (s, 3H), 2.64 (t, J = 7.4 Hz, 2H),

8.67 (s, 1H), 11.40 (br s, 1H)

HRMS (ESI, *m/z*, MH+) Calcd for $C_{11}H_{16}N_3$: 190.1339, Found: 190.1342

4.1.14. Synthesis of compound 16

Step1: 5-Bromo-4-chloro-2-methyl-7*H*-pyrrolo[2,3-*d*]pyrimidine (**54**)

To a suspension of 4-chloro-2-methyl-7*H*-pyrrolo[2,3-*d*]pyrimidine (**43**, 2.00 g, 11.9 mmol) in $CHCl_3$ (20 mL) was added *N*-bromosuccinimide (2.55 mg, 14.3 mmol). After stirring overnight at room temperature, the reactant mixture was quenched with saturated $NaHCO_3$ solution. The mixture was extracted with $CHCl_3$ and AcOEt, and the organic layer was washed with H_2O and brine, and dried over $MgSO_4$. After filtration and concentration, for purification, the residue was slurried in *n*-hexane/AcOEt (1/1 (v/v)). The precipitated solid was collected by filtration, washed with *n*-hexane, and dried to give the title compound **54** (2.50 g, approx. 70% yield) as a mixture of 15% of 5,6-dibromo-4-chloro-2-methyl-7*H*-pyrrolo[2,3-*d*]pyrimidine.

^{1}H NMR (400 MHz, DMSO-d_6) δ: 2.62 (s, 3H), 7.82 (d, J = 2.5 Hz, 1H), 12.69 (br s, 1H)

Step 2: 4-Chloro-2,5-dimethyl-7*H*-pyrrolo[2,3-*d*]pyrimidine (**55**)

To a solution of **54** (85% purity, 2.50 g, 8.70 mmol) in THF (45 mL), 1.63 M *n*-butyllithium in hexane (15.0 mL, 23.3 mmol) was added at −78 °C. After stirring for 1 h at −78 °C, methyl iodide (662 μL, 10.6 mmol) was added to the reactant mixture, and then the mixture was stirred at 0 °C for 1 h. The mixture was diluted with H_2O and extracted with AcOEt. The organic layer was washed with H_2O and brine, and dried over $MgSO_4$. After filtration and concentration, for purification, the residue was slurried in *n*-hexane/AcOEt (2/1 (v/v)). The precipitated solid was collected by filtration, washed with *n*-hexane, and dried to give the title compound **55** (660 mg, approx. 35% yield) as a mixture of 10% of 4-chloro-2-methyl-7*H*-pyrrolo[2,3-*d*]pyrimidine.

^{1}H NMR (400 MHz, DMSO-d_6) δ: 2.38 (br s, 3H), 2.58 (s, 3H), 7.30 (br s, 1H), 11.94 (br s, 1H)

Step 3: 4-Chloro-2,5-dimethyl-7-tosyl-7*H*-pyrrolo[2,3-*d*]pyrimidine (**56**)

Compound **55** (90% purity, 660 mg, 3.27 mmol) was added to a suspension of sodium hydride 60% dispersion in mineral oil (160 mg, 4.00 mmol) was dissolved in DMF (6.0 mL) at 0 °C. After stirring for 30 min at 0 °C, *p*-toluenesulfonyl chloride (762 mg, 3.99 mmol) was added to the solution at 0 °C, and the mixture was stirred at room temperature for 30 min. The mixture was diluted with H_2O and extracted with AcOEt, and the organic layer was washed with H_2O and brine, and dried over $MgSO_4$. After filtration and concentration, for purification, the residue was slurried in *n*-hexane. The precipitated solid was collected by filtration, washed with *n*-hexane, and dried to give the title compound **56** (1.00 g, 91% yield) which was applied to the next step without further purification.

Step 4: Ethyl 4-chloro-2,5-dimethyl-7-tosyl-7*H*-pyrrolo[2,3-*d*]pyrimidine-6-carboxylate (**57**)

To a solution of **56** (1.00 g, 2.98 mmol) in THF (10 mL), 1.55 M *n*-butyllithium in hexane (2.88 mL, 4.46 mmol) was added at −78 °C. After stirring for 3 h at −78 °C, ethyl chloroformate (426 μL, 4.46 mmol) was added to the reactant mixture, and then the mixture was stirred overnight at room temperature. The mixture was diluted with H_2O and 1 N HCl solution, and extracted with AcOEt. The organic layer was washed with H_2O and brine, and dried over $MgSO_4$. After filtration and concentration, the residue was purified by silica gel column chromatography (eluted with *n*-hexane/EtOAc = 90/10 to 80/20 (v/v)) to give the title compound **57** (560 mg, 46% yield) as a mixture containing a small amount of impurities. This was advanced to the next step without further purification.

Step 5: 4-Chloro-2,5-dimethyl-7*H*-pyrrolo[2,3-*d*]pyrimidine-6-carboxylic acid (**58**)

To a solution of **57** (560 mg, 1.37 mmol) in THF (5.0 mL), 1.0 M lithium hydroxide solution (6.00 mL, 6.00 mmol) was added. After stirring overnight at 50 °C, the mixture was diluted with H_2O. And then, the mixture was neutralized with 6.0 M aqueous HCl solution. Precipitated solid was collected by filtration, washed with H_2O, and dried to give the title compound **58** (300 mg, 97% yield) which was advanced to the next step without further purification.

Step 6: 4-Chloro-*N*,2,5-trimethyl-7*H*-pyrrolo[2,3-*d*]pyrimidine-6-carboxamide (**16**)

To a solution of **58** (100 mg, 0.443 mmol) in 1:1 $CHCl_3$-THF (2.0 mL) was added 1-(3-dimethylaminopropyl)-3-ethylcarbodiimide hydrochloride (169 mg, 0.886 mmol), *N,N*-dimethyl-4-aminopyridine (5.00 mg, 0.0409 mmol) and 40% methylamine in methanol (34.0 μg, 0.493 mmol), and the mixture was stirred overnight at room temperature. The mixture was diluted with H_2O and extracted with AcOEt. The organic layer was washed with H_2O, saturated aqueous $NaHCO_3$ solution and brine, and dried over $MgSO_4$. After filtration and concentration, for purification, the residue was slurried in AcOEt. The precipitated solid was collected by filtration, washed with a small portion of AcOEt, and dried to give the title compound **16** (73.0 mg, 69% yield).

^{1}H NMR (400 MHz, DMSO-d_6) δ: 2.60 (s, 3H), 2.61 (s, 3H), 2.81 (d, J = 4.6 Hz, 3H), 8.11 (br d, J = 4.6 Hz, 1H), 12.32 (br s, 1H)

HRMS (ESI, *m/z*, MH+) Calcd for $C_{10}H_{12}N_4Cl_1$: 239.0694, Found: 239.0688

4.1.15. Synthesis of compound 18

Step1: 4-Chloro-2-methyl-7-((2-(trimethylsilyl)ethoxy)methyl)-7*H*-pyrrolo[2,3-*d*]pyrimidine-6-carbaldehyde (**59**)

To a solution of **44** (1.50 g, 5.03 mmol) in THF (15 mL), 1.63 M *n*-butyllithium in hexane (4.01 mL, 6.54 mmol) was added at −78 °C. After stirring for 3 h at −78 °C, *N,N*-dimethylformamide (503 μL, 6.54 mmol) was added to the reactant mixture, and then the mixture was stirred at room temperature for 1 h. The mixture was diluted with H_2O and saturated aqueous NH_4Cl solution, and extracted with AcOEt. The organic layer was washed with H_2O and brine, and dried over $MgSO_4$. After filtration and concentration, the residue was loaded on silica gel column chromatography (eluted with *n*-hexane/EtOAc = 90/10 (v/v)) for elimination of the polar component. The title compound **59** (1.08 g, 66% yield) was obtained, which was applied to the next step without further purification.

Step 2: (E)-4-Chloro-2-methyl-6-(prop-1-en-1-yl)-7-((2-(trimethylsilyl)ethoxy)methyl)-7*H*-pyrrolo[2,3-*d*]pyrimidine (**60**)

Phenyllithium (2.1 M) in dibutyl ether (613 μL, 1.28 mmol) was added at 0 °C to a solution of ethyltriphenylphosphonium bromide (250 mg, 0.673 mmol) in THF (2.5 mL) and stirred for 15 min at 0 °C. The mixture was cooled to −78 °C and a solution **59** (200 mg, 0.613 mmol) in THF (2.5 mL) was added. After stirring at −78 °C for 30 min, additional 2.1 M phenyllithium in dibutyl ether (292 μL, 0.613 mmol) was added to the mixture, and then stirred for another 1.5 h at −78 °C. The reactant mixture was diluted with H_2O and saturated aqueous NH_4Cl solution, and extracted with AcOEt. The organic layer was washed with H_2O and brine, and dried over $MgSO_4$. After filtration and concentration, the residue was purified by preparative TLC (*n*-hexane/AcOEt = 4/1 (v/v)) to give the title compound **60** (50.0 mg, 24% yield).

^{1}H NMR (400 MHz, DMSO-d_6) δ: −0.11 (s, 9H), 0.80–0.88 (m. 2H), 1.93 (d, J = 4.6 Hz, 3H), 2.63 (s, 3H), 3.46–3.52 (m, 2H), 5.65 (s, 2H), 6.64–6.66 (m, 2H), 6.77 (s, 1H)

Step 3: (E)-4-Chloro-2-methyl-6-(prop-1-en-1-yl)-7*H*-pyrrolo[2,3-*d*]pyrimidine (**61**)

Compound **60** (50 mg, 0.153 mmol) was dissolved in 1:1 $CHCl_3$-TFA (2.0 mL), and the mixture was stirred at room temperature for 1 h. After evaporation of $CHCl_3$ and TFA, the residue was diluted with THF and neutralized with 2 N NaOH solution, and then extracted with AcOEt. The organic layer was washed with H_2O, 1 N HCl solution and brine, and dried over $MgSO_4$. After filtration and concentration, for purification, the residue was slurried in *n*-hexane/AcOEt (10/1 (v/v)). The precipitated solid was collected by filtration, washed with *n*-hexane, and dried to give the title compound **61** (20.0 mg, 65% yield).

^{1}H NMR (400 MHz, DMSO-d_6) δ: 1.89 (d, J = 5.5 Hz, 3H), 2.59 (s, 3H), 6.38–6.58 (m, 3H), 12.37 (br s, 1H)

Step 4: (E)-4,5-Dichloro-2-methyl-6-(prop-1-en-1-yl)-7*H*-pyrrolo[2,3-*d*]pyrimidine (**18**)

To a solution of **61** (10.0 mg, 4.82 × 10^{-2} mmol) in DMF (1.0 mL) was added *N*-chlorosuccinimide (10.0 mg, 7.49 × 10^{-2} mmol). After stirring overnight at room temperature, the reactant mixture was quenched with saturated $NaHCO_3$ solution. The mixture was extracted with AcOEt, and the organic layer was washed with H_2O and brine, and dried over $MgSO_4$. After filtration and concentration, the residue was purified by preparative TLC (*n*-hexane/AcOEt = 1/1 (v/v)) to give the title compound **18** (5.0 mg, 43% yield).

^{1}H NMR (400 MHz, $CDCl_3$) δ: 2.00 (dd, J = 6.7, 1.7 Hz, 3H), 2.73 (s, 3H), 6.23 (dq, J = 16.1, 6.7 Hz, 1H), 6.58 (dq, J = 16.1, 1.7 Hz, 1H), 9.57 (br s, 1H)

HRMS (ESI, *m/z*, MH+) Calcd for $C_{10}H_{10}N_3Cl_2$: 242.0246, Found: 242.0527

4.1.16. Synthesis of compound 17

Step 1: 4-Chloro-2-methyl-7-((2-(trimethylsilyl)ethoxy)methyl)-7*H*-pyrrolo[2,3-*d*]pyrimidine-6-carboxylic acid (**62**)

Sodium dihydrogen phosphate dihydrate (114 mg, 0.734 mmol), 2-methylbut-2-ene (650 μg, 6.14 mmol) and sodium chlorite (68.0 mg, 0.736 mmol) were sequentially added to a solution of **59** (200 mg, 0.613 mmol) in 2:2:1 *t*-BuOH-H_2O-THF (2.5 mL) and stirred overnight at room temperature. The reactant mixture was diluted with H_2O and extracted with AcOEt. The organic layer was washed with H_2O and brine, and dried over $MgSO_4$. After filtration and concentration, for purification, the residue was slurried in *n*-hexane. The precipitated solid was collected by filtration, washed with *n*-hexane, and dried to give the title compound **62** (120 mg, 57% yield) as a mixture with a small amount of impurities. This was used for the next step without further purification.

Step 2: 4-Chloro-*N*,2-dimethyl-7-((2-(trimethylsilyl)ethoxy)methyl)-7*H*-pyrrolo[2,3-*d*]pyrimidine-6-carboxamide (**63**)

To a solution of **62** (120 mg, 0.350 mmol) in $CHCl_3$ (2.0 mL) was added 1-(3-dimethylaminopropyl)-3-ethylcarbodiimide hydrochloride (74.0 mg, 0.386 mmol), N,*N*-dimethyl-4-aminopyridine (2.00 mg, 0.0164 mmol) and 40% methylamine in methanol (39.0 μL, 0.386 mmol), and the mixture was stirred overnight at room temperature. The mixture was diluted with H_2O and extracted with AcOEt. The organic layer was washed with H_2O, saturated aqueous $NaHCO_3$ solution and brine, and dried over $MgSO_4$. After filtration and concentration, the residue was loaded on silica gel column chromatography (eluted with *n*-hexane/EtOAc = 66/34 (v/v)) for elimination of the polar component. The title compound **63** (90.0 mg, 72% yield) was obtained, which was used for the next step without further purification.

Step 3: 5-Bromo-4-chloro-*N*-2-dimethyl-7-((2-(trimethylsilyl)ethoxy)methyl)-7*H*-pyrrolo[2,3-*d*]pyrimidine-6-carboxamide (**64**)

To a suspension of **63** (90.0 mg, 0.253 mmol) in $CHCl_3$ (2.0 mL) was added *N*-bromosuccinimide (54.0 mg, 0.304 mmol). After stirring at room temperature for 2.5 h, the reactant mixture was quenched with saturated $NaHCO_3$ solution. The mixture was extracted with AcOEt, and the organic layer was washed with H_2O and brine, and dried over $MgSO_4$. After filtration and concentration, the residue was purified by preparative TLC (*n*-hexane/AcOEt = 2/1 (v/v)) to give the title compound **64** (92.0 mg, 84% yield) as a mixture with a small amount of impurities. This mixture was used for the next step without further purification.

Step 4: 5-Bromo-4-chloro-*N*-2-dimethyl-7*H*-pyrrolo[2,3-*d*]pyrimidine-6-carboxamide (**17**)

To a solution of **64** (90.0 mg, 0.207 mmol) in CH_2Cl_2 (1.0 mL), boron trifluoride diethyl etherate (77.0 μL, 0.624 mmol) was added at room temperature. After stirring overnight at room temperature, the mixture was quenched with 2 N NaOH solution and extracted with AcOEt. The organic layer was washed with H_2O and brine, and dried over $MgSO_4$. After filtration and concentration, for purification, the residue was slurried in AcOEt. The precipitated solid was collected by filtration, washed with *n*-hexane, and dried to give the title compound **17** (49.0 mg, 77% yield).

^{1}H NMR (400 MHz, DMSO-d_6) δ: 2.63 (s, 3H), 2.84 (d, J = 4.4 Hz, 3H), 8.29 (q, J = 4.4 Hz, 1H), 13.17 (br s, 1H)

HRMS (ESI, *m/z*, MH+) Calcd for $C_9H_9O_1N_4Br_1Cl_2$: 302.9643, Found: 302.9636

4.2. Crystallographic methods

Protein production and purification of PDHK4 kinase domain (residues 10–411) and PDHK2 kinase domain (residues 16–407) were carried out as previously reported.[16–17] Briefly, these PDHK kinase domains were produced in *Escherichia coli* and purified by Ni-NTA affinity column, protease digestion and gel filtration. The purified PDHK4 proteins were crystallized and crystals were obtained at 22 °C using the hanging-drop vapor diffusion method with reservoir containing 50 mM $KHPO_4$ pH 7.5, 1.7 M ammonium sulfate and 4% (v/v) PEG400, 5 mM ADP. X-ray fragment screening was carried out using in-house fragment library. A soaking drop was prepared by adding the cocktail mixture of four fragments to achieve a final concentration of 12.5 mM. Crystals were then transferred to the soaking drop and soaked for a period of 24 h. For SBDD studies of PDHK4 in complex with fragment hit derivatives, structures of these complexes with compounds **1**, **3**, and **7** were obtained by soaking in a similar manner. Regarding PDHK2, the purified PDHK2 proteins were crystallized in complex with compound **13**. Co-crystals were obtained at 4 °C using the hanging-drop vapor diffusion method with reservoir containing 50 mM Na acetate pH 5.5, 100 mM magnesium chloride and 8% (v/v) isopropanol.

Diffraction data of the soaked crystals and co-crystals were collected at Photn Factory (Japan), SPring-8 (Japan), Canadian Light Source (Canada) and Swiss Light Source (Switzerland). The data were integrated with DIALS and scaled using aimless.[18] The structures of the PDHK-compound complex were solved by molecular replacement with MOLREP in CCP4 suite[19–20] using the coordinates of the PDHK4 kinase domain (PDB ID 2ZKJ[16]) or the PDHK2 kinase domain (PDB ID 2BTZ[17]) as the model. The structural models were built in Coot[21] and refined using REFMAC5 in CCP4 suite[22] and Phenix[23]. Figures were created using PyMOL[24].

4.3. Spectrophotometry assay to measure the inhibitory activity on PDHKs

PDHK activity was assessed indirectly by measuring the residual PDH activity after PDHK reaction essentially as described previously.[25] Briefly, a porcine PDH complex (Sigma-Aldrich) and each of the recombinant human PDHK (1, 2, 3, or 4) enzymes were mixed and incubated overnight at 4 °C to obtain PDH/PDHK complex. The PDH/PDHK complex and PDHK inhibitors were incubated for 45 min at room temperature after adding 0.3 or 10 μM ATP to start the PDHK reaction. Then, the substrates for PDH (5.0 mM coenzyme A, 5.0 mM sodium pyruvate and 12 mM β-nicotinamide adenine dinucleotide) were added to start the PDH reaction and incubated for 90 min at room temperature. The PDH reaction was analyzed by measuring the reaction product, NADH. The amount of NADH was determined measuring the absorbance at 340 nm before and after the PDH reaction. Concentration − response data were fitted to the following equation using Spotfire (TIBCO):

$$\%\text{inhibition} = (\text{max - min})/\ 1 + 10^{(\log \text{IC50 - log [comp]}) \times \text{Hill}} + \text{min}$$

where min is the 100% enzymatic activity control, max is the 0% enzymatic activity control.

4.4. RapidFire MS assay to measure the inhibitory activity on PDHK2 and PDHK4

The PDH reaction mixtures were diluted 25 fold with 0.1% (v/v) formic acid. The PDH reaction product acetyl-coenzyme A was subsequently analyzed using RapidFire300 (Agilent TechnologiShes), an integrated high throughput autosampler/solid-phase extraction system, coupled to a 3200QTRAP triple-quadrupole mass spectrometer (Sciex). The samples were aspirated under vacuum directly from 384-well assay plates for 0.25 s and loaded onto a graphitic carbon (Type D) solid-phase extraction cartridge (Agilent Technologies) with 5 mM ammonium acetate (pH 10.0) at a flow rate of 1.25 mL/min for 3 s. Acetyl-coenzyme A was eluted with a 5 mM ammonium acetate (pH 10.0) /acetonitrile/acetone mixture (50:25:25, v/v/v) at a rate of 1.5 mL/min for 5 s. The cartridge was then re-equilibrated with 5 mM ammonium acetate (pH 10.0) at a rate of 1.25 mL/min for 0.5 s. The eluate was analyzed in the mass spectrometer in the positive ionization mode using a gas temperature of 350 °C, a nebulizer pressure of 50 psi, and a spray voltage of 5500 V. The mass spectrometer was operated in the multiple reaction monitoring (MRM) mode, with transitions (Q1/Q3) of analyte as follows: 808/79 and 808/408. The area under the curve (AUC) of the extracted ion counts was calculated using RapidFire Integrator version 3.6 (Agilent Technologies). MS/MS signal of ATP was used to confirm every introduction of a sample into the mass spectrometer.

4.5. Fluorescence polarization assay on HSP90

The measurement of inhibitory activity of HSP90 was performed using the assay kit from BPS Bioscience (catalog number: 50293).

4.6. Luminescent assay to measure the inhibitory activity on BCKDK

BCKDK activity was assessed by ADP-Glo™ Kinase Assay (Promega Corporation). Human recombinant BCKDK and PDHK inhibitors were incubated for 60 min at 37 °C after adding 0.2 μM ATP to start the BCKDK reaction. ADP-Glo™ Reagent were added and incubated for 40 min at room temperature to terminate the kinase reaction and deplete the remaining ATP. Then, Kinase Detection Reagent was added and incubated for 40 min at room temperature to convert ADP to ATP. The amount of ATP was determined measuring luminescence.

Concentration − response data were fitted to the following equation using Spotfire (TIBCO):

$$\%\text{inhibition} = (\text{max - min})/\ 1 + 10^{(\log IC50\ -\ \log [comp])\ x\ Hill} + \text{min}$$

where min is the 100% enzymatic activity control, max is the 0% enzymatic activity control.

4.7. Kinase selectivity assay

The kinase panel assay was conducted using the DiscoveRx KINOME scan™ assay service toward 59 kinases.

4.8. Computational study

WaterMap (Schrödinger Release 2018–1: Schrödinger, LLC, New-York, NY, 2018) calculations were performed on the co-crystal structure of fragment hit **1** bound to PDHK4. Input structure was prepared by Protein Preparation Wizard in Maestro (Schrödinger Release 2018–1) using default options. WaterMap was run in default mode with OPLS3e force fields, existing waters were deleted, and a 2 ns MD simulation. The fragment hit **1** was used to define the binding site.

5. Accession codes

Atomic coordinates and structure factors have been deposited in the Protein Data Bank with codes 7EAT for **1**/PDHK4, 7EBB for **2**/PDHK4, 7EA0 for **1**/PDHK2, 7EAS for **2**/PDHK2, 7EBG for **7**/PDHK4 and 7EBH for **13**/PDHK2 respectively.

Declaration of Competing Interest

The authors declare that they have no known competing financial interests or personal relationships that could have appeared to influence the work reported in this paper.

Acknowledgments

The authors thank Mr. Eita Nagao for analytical support, and Dr. Jiro Kataoka for helpful discussion. We also thank Prof. Toshiya Senda for the data collection at the Photon Factory, KEK.

Appendix A. Supplementary material

Supplementary data to this article can be found online at https://doi.org/10.1016/j.bmc.2021.116283.

References

1 Golias T, Kery M, Radenkovic S, Papandreou I. Microenvironmental control of glucose metabolism in tumors by regulation of pyruvate dehydrogenase. *Int J Cancer*. 2019;144:674–686. https://doi.org/10.1002/ijc.31812.
2 Rowles J, Scherer SW, Xi T, et al. Cloning and characterization of PDK4 on 7q21.3 encoding a fourth pyruvate dehydrogenase kinase isoenzyme in human. *J Biol Chem*. 1996;271:22376–22382. https://doi.org/10.1074/jbc.271.37.22376.
3 Kulkarni SS, Salehzadeh F, Fritz T, Zierath JR, Krook A, Osler ME. Mitochondrial regulators of fatty acid metabolism reflect metabolic dysfunction in type 2 diabetes mellitus. *Metabolism*. 2012;61:175–185. https://doi.org/10.1016/j.metabol.2011.06.014.
4 Piao L, Sidhu VK, Fang YH, et al. FOXO1-mediated upregulation of pyruvate dehydrogenase kinase-4 (PDK4) decreases glucose oxidation and impairs right ventricular function in pulmonary hypertension: therapeutic benefits of dichloroacetate. *J Mol Med*. 2013;91:333–346. https://doi.org/10.1007/s00109-012-0982-0.
5 Mori J, Alrob OA, Wagg CS, Harris RA, Lopaschuk GD, Oudit GY. ANG II causes insulin resistance and induces cardiac metabolic switch and inefficiency: a critical role of PDK4. *Am J Physiol - Hear Circ Physiol*. 2013;304:1103–1113. https://doi.org/10.1152/ajpheart.00636.2012.
6 Bonnet S, Archer SL, Allalunis-Turner J, et al. A mitochondria-K+ channel axis is suppressed in cancer and its normalization promotes apoptosis and inhibits cancer growth. *Cancer Cell*. 2007;11:37–51. https://doi.org/10.1016/j.ccr.2006.10.020.
7 Korotchkina LG, Patel MS. Site specificity of four pyruvate dehydrogenase kinase isoenzymes toward the three phosphorylation sites of human pyruvate dehydrogenase. *J Biol Chem*. 2001;276:37223–37229. https://doi.org/10.1074/jbc.M103069200.
8 Jeoung NH, Rahimi Y, Wu P, Lee WNP, Harris RA. Fasting induces ketoacidosis and hypothermia in PDHK2/PDHK4-double-knockout mice. *Biochem J*. 2012;443:829–839. https://doi.org/10.1042/BJ20112197.
9 Wei Q, Xia Y. Roles of 3-phosphoinositide-dependent kinase 1 in the regulation of endothelial nitric-oxide synthase phosphorylation and function by heat shock protein 90. *J Biol Chem*. 2005;280:18081–18086. https://doi.org/10.1074/jbc.M413607200.
10 Brough PA, Baker L, Bedford S, et al. Application of off-rate screening in the identification of novel pan-isoform inhibitors of pyruvate dehydrogenase kinase. *J Med Chem*. 2017;60:2271–2286. https://doi.org/10.1021/acs.jmedchem.6b01478.
11 Tso SC, Qi X, Gui WJ, et al. Structure-guided development of specific pyruvate dehydrogenase kinase inhibitors targeting the ATP-binding pocket. *J Biol Chem*. 2014;289:4432–4443. https://doi.org/10.1074/jbc.M113.533885.
12 Tso SC, Lou M, Wu CY, et al. Development of dihydroxyphenyl sulfonylisoindoline derivatives as liver-targeting pyruvate dehydrogenase kinase inhibitors. *J Med Chem*. 2017;60:1142–1150. https://doi.org/10.1021/acs.jmedchem.6b01540.
13 Kukimoto-Niino M, Tokmakov A, Terada T, et al. Inhibitor-bound structures of human pyruvate de-hydrogenase kinase 4. *Acta Cryst*. 2011;D67:763–773. https://doi.org/10.1107/S090744491102405X.
14 Ferreira LG, Andricopulo AD, et al. From protein structure to small-molecules: recent advances and applications to fragment-based drug discovery. *Current Top Med Chem*. 2017;17:2260–2270. https://doi.org/10.2174/1568026617666170224113437.
15 Abel Robert, Mondal Sayan, Masse Craig, et al. Accelerating drug discovery through tight integration of expert molecular design and predictive scoring. *Curr Opin Struct Biol*. 2017;43:38–44. https://doi.org/10.1016/j.sbi.2016.10.007.
16 Wynn RM, Kato M, Chuang JL, Tso SC, Li J, Chuang DT. Pyruvate dehydrogenase kinase-4 structures reveal a metastable open conformation fostering robust core-free basal activity. *J Biol Chem*. 2008;283:25305–25315. https://doi.org/10.1074/jbc.M802249200.
17 Knoechel TR, Tucker AD, Robinson CM, et al. Regulatory roles of the N-terminal domain based on crystal structures of human pyruvate dehydrogenase kinase 2

containing physiological and synthetic ligands. *Biochemistry*. 2006;45:402–415. https://doi.org/10.1021/bi051402s.
18 Winter G, Waterman DG, Parkhurst JM, et al. DIALS: Implementation and evaluation of a new integration package. *Acta Crystallogr Sect D Struct Biol*. 2018;74:85–97. https://doi.org/10.1107/S2059798317017235.
19 Evans PR, Murshudov GN. How good are my data and what is the resolution? *Acta Crystallogr Sect D Biol Crystallogr*. 2013;69:1204–1214. https://doi.org/10.1107/S0907444913000061.
20 Vagin A, Teplyakov A. MOLREP: an automated program for molecular replacement. *J Appl Crystallogr*. 1997;30:1022–1025. https://doi.org/10.1107/S0021889897006766.
21 Winn MD, Ballard CC, Cowtan KD, et al. Overview of the CCP4 suite and current developments. *Acta Crystallogr Sect D Biol Crystallogr*. 2011;67:235–242. https://doi.org/10.1107/S0907444910045749.
22 Emsley P, Cowtan K. Coot: model-building tools for molecular graphics. *Acta Crystallogr Sect D Biol Crystallogr*. 2004;60:2126–2132. https://doi.org/10.1107/S0907444904019158.
23 Murshudov GN, Skubák P, Lebedev AA, et al. REFMAC5 for the refinement of macromolecular crystal structures. *Acta Crystallogr Sect D Biol Crystallogr*. 2011;67:355–367. https://doi.org/10.1107/S0907444911001314.
24 Liebschner D, Afonine PV, Baker ML, et al. Macromolecular structure determination using X-rays, neutrons and electrons: recent developments in Phenix. *Acta Crystallogr Sect D Struct Biol*. 2019;75:861–877. https://doi.org/10.1107/S2059798319011471.
25 Jackson JC, Vinluan CC, Dragland CJ, et al. Heterologously expressed inner lipoyl domain of dihydrolipoyl acetyltransferase inhibits ATP-dependent inactivation of pyruvate dehydrogenase complex: identification of important amino acid residues. *Biochem J*. 1998;334:703–711. https://doi.org/10.1042/bj3340703.